Taylor & Francis
Taylor & Francis Group

RESEARCH ARTICLE

Advances in molecular quantum chemistry contained in the Q-Chem 4 program package

Yihan Shao[a], Zhengting Gan[a], Evgeny Epifanovsky[a,b,c], Andrew T.B. Gilbert[d], Michael Wormit[e], Joerg Kussmann[f], Adrian W. Lange[g], Andrew Behn[c], Jia Deng[d], Xintian Feng[b], Debashree Ghosh[b,1], Matthew Goldey[c], Paul R. Horn[c], Leif D. Jacobson[g], Ilya Kaliman[h], Rustam Z. Khaliullin[c], Tomasz Kuś[b], Arie Landau[b,2], Jie Liu[i,g], Emil I. Proynov[a,3], Young Min Rhee[c,4], Ryan M. Richard[g], Mary A. Rohrdanz[g,5], Ryan P. Steele[j], Eric J. Sundstrom[c], H. Lee Woodcock III[ad], Paul M. Zimmerman[c,k], Dmitry Zuev[b], Ben Albrecht[l], Ethan Alguire[s], Brian Austin[c], Gregory J. O. Beran[m], Yves A. Bernard[b], Eric Berquist[l], Kai Brandhorst[c,6], Ksenia B. Bravaya[b,7], Shawn T. Brown[a,8], David Casanova[c,n], Chun-Min Chang[a], Yunqing Chen[k], Siu Hung Chien[a], Kristina D. Closser[a], Deborah L. Crittenden[d,9], Michael Diedenhofen[o], Robert A. DiStasio Jr.[c], Hainam Do[p], Anthony D. Dutoi[q], Richard G. Edgar[r], Shervin Fatehi[s,j], Laszlo Fusti-Molnar[a,10], An Ghysels[t,11], Anna Golubeva-Zadorozhnaya[b], Joseph Gomes[c], Magnus W.D. Hanson-Heine[p], Philipp H.P. Harbach[e], Andreas W. Hauser[c], Edward G. Hohenstein[u], Zachary C. Holden[g], Thomas-C. Jagau[b], Hyunjun Ji[v], Benjamin Kaduk[w], Kirill Khistyaev[b], Jaehoon Kim[v], Jihan Kim[c,12], Rollin A. King[x], Phil Klunzinger[y], Dmytro Kosenkov[h,13], Tim Kowalczyk[w,14], Caroline M. Krauter[e], Ka Un Lao[g], Adèle D. Laurent[b,15], Keith V. Lawler[c,16], Sergey V. Levchenko[b,17], Ching Yeh Lin[d], Fenglai Liu[al], Ester Livshits[z], Rohini C. Lochan[c], Arne Luenser[f], Prashant Manohar[b,18], Samuel F. Manzer[c], Shan-Ping Mao[aa], Narbe Mardirossian[c], Aleksandr V. Marenich[ab], Simon A. Maurer[f], Nicholas J. Mayhall[c], Eric Neuscamman[c], C. Melania Oana[b], Roberto Olivares-Amaya[r,ac], Darragh P. O'Neill[d], John A. Parkhill[c,19], Trilisa M. Perrine[k,20], Roberto Peverati[ab,c], Alexander Prociuk[k], Dirk R. Rehn[e], Edina Rosta[b,21], Nicholas J. Russ[a], Shaama M. Sharada[c], Sandeep Sharma[ac], David W. Small[c], Alexander Sodt[c,t], Tamar Stein[z,5], David Stück[c], Yu-Chuan Su[aa], Alex J.W. Thom[c,22], Takashi Tsuchimochi[w], Vitalii Vanovschi[b], Leslie Vogt[r], Oleg Vydrov[w], Tao Wang[b], Mark A. Watson[ac,r], Jan Wenzel[e], Alec White[c], Christopher F. Williams[g], Jun Yang[ac], Sina Yeganeh[w], Shane R. Yost[c,w], Zhi-Qiang You[ae,g], Igor Ying Zhang[af], Xing Zhang[g], Yan Zhao[ab], Bernard R. Brooks[t], Garnet K.L. Chan[ac], Daniel M. Chipman[ag], Christopher J. Cramer[ab], William A. Goddard III[ah], Mark S. Gordon[ai], Warren J. Hehre[y], Andreas Klamt[o], Henry F. Schaefer III[aj], Michael W. Schmidt[ai], C. David Sherrill[u], Donald G. Truhlar[ab], Arieh Warshel[b], Xin Xu[af], Alán Aspuru-Guzik[r], Roi Baer[z], Alexis T. Bell[c], Nicholas A. Besley[p], Jeng-Da Chai[aa], Andreas Dreuw[e], Barry D. Dunietz[ak], Thomas R. Furlani[al], Steven R. Gwaltney[am], Chao-Ping Hsu[ae], Yousung Jung[v], Jing Kong[a,3], Daniel S. Lambrecht[l], WanZhen Liang[i], Christian Ochsenfeld[f], Vitaly A. Rassolov[an], Lyudmila V. Slipchenko[h], Joseph E. Subotnik[s], Troy Van Voorhis[w], John M. Herbert[g], Anna I. Krylov[b], Peter M.W. Gill[d] and Martin Head-Gordon[c,*]

[a]Q-Chem Inc, Pleasanton, CA, USA; [b]Department of Chemistry, University of Southern California, Los Angeles, CA, USA; [c]Department of Chemistry, University of California, Berkeley, CA, USA; [d]Research School of Chemistry, Australian National University, Canberra, Australia; [e]Interdisciplinary Center for Scientific Computing, Ruprecht-Karls University, Heidelberg, Germany; [f]Department of Chemistry, University of Munich (LMU), München, Germany; [g]Department of Chemistry and Biochemistry, The Ohio State University, Columbus, OH, USA; [h]Department of Chemistry, Purdue University, West Lafayette, IN, USA; [i]Department of Chemistry, Xiamen University, Xiamen, China; [j]Department of Chemistry, The University of Utah, Salt Lake City, UT, USA; [k]Department of Chemistry, University of Michigan, Ann Arbor, MI, USA; [l]Department of Chemistry, University of Pittsburgh, Pittsburgh, PA, USA; [m]Department of Chemistry, University of California, Riverside, CA, USA; [n]IKERBASQUE - Basque Foundation for Science & Donostia International Physics Center (DIPC) & Kimika Fakultatea, Euskal Herriko Unibertsitatea (UPV/EHU), Donostia, Spain; [o]COSMOlogic GmbH & Co. KG, Leverkusen, Germany; [p]School of Chemistry, The University of Nottingham, Nottingham, United Kingdom; [q]Department of Chemistry, University of the Pacific, Stockton, CA, USA; [r]Department of Chemistry and Chemical Biology, Harvard University, Cambridge, MA, USA; [s]Department of Chemistry, University of Pennsylvania, Philadelphia, PA, USA; [t]Computational Biophysics Section, Heart, Lung, and Blood Institute, National Institutes of Health, Bethesda, MD, USA; [u]School of Chemistry and Biochemistry, Georgia Institute of Technology, Atlanta, GA, USA; [v]Graduate School of EEWS, KAIST, Daejeon, Republic of Korea; [w]Department of Chemistry, Massachusetts Institute of Technology, Cambridge, MA, USA; [x]Department of Chemistry, Bethel University, St. Paul, MN, USA; [y]Wavefunction Inc., Irvine, CA, USA; [z]The Chaim Weizmann Institute of Chemistry, and the Fritz Haber Research Center for Molecular Dynamics, The Hebrew University of Jerusalem, Jerusalem, Israel; [aa]Department of Physics, National Taiwan University, Taipei, Taiwan; [ab]Department of Chemistry, University of Minnesota, Minneapolis, MN, USA; [ac]Department of Chemistry, Princeton University, Princeton, NJ, USA; [ad]Department of Chemistry, University of South Florida, Tampa, FL, USA; [ae]Institute of Chemistry, Academia Sinica, Taipei, Taiwan; [af]Department of Chemistry, Fudan University, Shanghai, China; [ag]Radiation Laboratory, University of Notre Dame, Notre Dame, IN, USA; [ah]Materials and Process Simulation Center, California Institute of Technology, Pasadena, CA, USA; [ai]Department of Chemistry, Iowa State University, Ames, IA, USA; [aj]Department of Chemistry, University of Georgia, Athens, GA, USA; [ak]Department of Chemistry and Biochemistry, Kent State University, Kent, OH, USA; [al]Center for Computational Research, SUNY at Buffalo, Buffalo, NY, USA; [am]Department of Chemistry, Mississippi State University, Mississippi State, MS, USA; [an]Department of Chemistry and Biochemistry, University of South Carolina, Columbia, SC, USA

A summary of the technical advances that are incorporated in the fourth major release of the Q-CHEM quantum chemistry program is provided, covering approximately the last seven years. These include developments in density functional theory methods and algorithms, nuclear magnetic resonance (NMR) property evaluation, coupled cluster and perturbation theories, methods for electronically excited and open-shell species, tools for treating extended environments, algorithms for walking on potential surfaces, analysis tools, energy and electron transfer modelling, parallel computing capabilities, and graphical user interfaces. In addition, a selection of example case studies that illustrate these capabilities is given. These include extensive benchmarks of the comparative accuracy of modern density functionals for bonded and non-bonded interactions, tests of attenuated second order Møller–Plesset (MP2) methods for intermolecular interactions, a variety of parallel performance benchmarks, and tests of the accuracy of implicit solvation models. Some specific chemical examples include calculations on the strongly correlated Cr_2 dimer, exploring zeolite-catalysed ethane dehydrogenation, energy decomposition analysis of a charged ter-molecular complex arising from glycerol photoionisation, and natural transition orbitals for a Frenkel exciton state in a nine-unit model of a self-assembling nanotube.

Keywords: quantum chemistry; software; electronic structure theory; density functional theory; electron correlation; computational modelling; Q-CHEM

Introduction

Quantum chemistry is a vigorous branch of theoretical chemistry, which is concerned with the development of practical theory, algorithms, and software, based on approximations to the fundamental principles of quantum mechanics (QM). While the electronic Schrödinger equation offers an in-principle exact description of the behaviour of electrons in molecules, subject to neglect of relativistic effects and nuclear motion, it is intractable to solve for realistic systems without approximations. Several fundamental approaches to developing such approximations have been followed. The predominant methods for present-day applications to larger molecules are based on the framework of density functional theory (DFT). For smaller molecules, accuracy that is higher can be achieved by the use of wave function theory approaches such as perturbation theory, and coupled cluster (CC) theories. The optimal model for a given problem depends on the accuracy required, the

[*]Corresponding author. Email: mhg@cchem.berkeley.edu

[1] Current address: Physical and Materials Chemistry Division, CSIR-National Chemical Laboratory, Pune 411008, India

[2] Current address: Faculty of Chemistry, Technion - Israel Institute of Technology, Technion City, Haifa 3200008, Israel

[3] Current address: Department of Chemistry, Middle Tennessee State University, 1301 East Main Street, Murfreesboro, TN 37132, USA

[4] Current address: Department of Chemistry, Pohang University of Science and Technology (POSTECH), Pohang, 790-784, Republic of Korea

[5] Current address: Department of Chemistry, Rice University, Houston, TX 77251, USA

[6] Current address: Institut für Anorganische und Analytische Chemie, Technische Universität Braunschweig, 38106 Braunschweig, Germany

[7] Current address: Department of Chemistry, Boston University, Boston, MA 02215, USA

[8] Current address: Pittsburgh Supercomputing Center, 300 S. Craig Street, Pittsburgh, PA 15213, USA

[9] Current address: Department of Chemistry, University of Canterbury, Christchurch, New Zealand

[10] Current address: OpenEye Scientific Software, 9 Bisbee Court, Suite D, Santa Fe, NM 87508, USA

[11] Current address: Center for Molecular Modeling, QCMM Alliance Ghent-Brussels, Ghent University, Technologiepark 903, B-9052 Zwijnaarde, Belgium

[12] Current address: Department of Chemical and Biomolecular Engineering, KAIST, Daejeon 305-701, Republic of Korea

[13] Current address: Department of Chemistry and Physics, Monmouth University, West Long Branch, New Jersey, 07764, USA

[14] Current address: Department of Chemistry, Western Washington University, 516 High St, Bellingham, WA 98225., USA

[15] Current address: University of Nantes, CEISAM UMR 6230 2 rue de la Houssinière, 44322 Nantes Cedex 1, France

[16] Current address: Department of Chemistry, University of Nevada, Las Vegas, NV 89154, USA

[17] Current address: Fritz-Haber-Institut der Max-Planck-Gesellschaft, Faradayweg 4-6, D-14195 Berlin, Germany

[18] Current address: Birla Institute of Technology and Science, Pilani 333031, Rajasthan, India

[19] Current address: Department of Chemistry, and Biochemistry, University of Notre Dame, Notre Dame, IN 46556, USA

[20] Current address: Department of Chemistry and Biochemistry, Ohio Northern University, Ada, OH 45810, USA

[21] Current address: Department of Chemistry, King's College London, London SE1 1DB, United Kingdom

[22] Current address: Department of Chemistry, Cambridge University, Lensfield Road, Cambridge CB2 1EW, United Kingdom

computational resources available, and the size of the system under consideration. In general, useful electronic structure methods trade off accuracy against computational feasibility over a very wide range.

All of the approximate methods of quantum chemistry provide models by which the electronic potential energy of a molecule, $E(\mathbf{R})$, can be evaluated as a function of the clamped nuclear positions, $\mathbf{R}$. Walking on the potential energy surface downwards to local minima leads to stable molecular structures, whose relative energies may be evaluated to predict reaction energies, and thus the thermodynamics of chemical transformations. Walking downhill in all directions but one (the reaction coordinate), and walking uphill in that direction leads to the first-order saddle points that separate reactants from products, and often play a major role in determining the kinetics of chemical reactions. Multi-step reaction mechanisms can in principle be identified this way, with the aid of appropriate surface-walking algorithms. Molecular properties, many of which can be used for spectroscopic characterisation, may also be evaluated from quantum chemical models as derivatives of the energy with respect to applied perturbations, such as electric fields or magnetic fields.

Putting together a useful range of quantum chemical models that offer different trade-offs between achievable accuracy and computational effort for a range of molecular sizes is a non-trivial matter. Things are further complicated by the need to evaluate a range of responses of the energy to such key perturbations as moving the atoms, and applying fields. Therefore, the realisation of electronic structure simulations through useful software has evolved over the past five decades into team science of increasingly large scale. Early efforts such as Gaussian 70 represented essentially the work of a single group (Sir John Pople's group). Today, there are roughly a dozen or so leading electronic structure codes in chemistry, all of which represent the end result of delocalised collaborations amongst many groups. In addition to Q-CHEM, and its collaborator, Spartan (www.wavefun.com), leading commercial programs are represented by the ADF program [1], the Gaussian program [2], Jaguar [3], MolCAS [4], the Molpro package [5], and the TURBOMOLE program [6,7]. In addition there is a range of non-commercial programs which also represent the result of substantial collaborations. These include ACES III [8], CFOUR [9], Dalton [10], GAMESS US [11] and UK [12], NWChem [13], and Psi [14]. Many other related codes exist in the condensed matter physics community, where periodic rather than molecular systems are typically the primary focus.

Some 21 years ago, in late 1992, Peter Gill, then a postdoctoral researcher with John Pople, began writing the first lines of a then-new quantum chemistry program, called Q-CHEM, over his Christmas vacation. This paper marks the fourth major release of the resulting software, which now is over 3 million lines of code, and contains a very wide range of functionality for calculating the structure and properties of molecules using methods based on the principles of QM. The technical developments prior to 2000 were summarised in a first major review on Q-CHEM version 2 [15], whose author list also illustrates the rapid growth in the number of contributors, which included not only members of the early founders' groups, but also many new groups including most famously the 1998 Nobel Laureate, Sir John Pople [16]. Subsequent advances between 2000 and 2006 were contained in Q-CHEM version 3.0, and were also documented in a review [17].

A very recent overview of Q-CHEM [18] provides some further details of the historical development and evolution of the package, as well as a high-level summary of its capabilities. Today Q-CHEM serves the needs of a very large number of users (over 50,000 including both direct users, and the very large number of users who access its capabilities as the back-end of the widely used Spartan modelling package). Q-CHEM also serves the needs of one of the larger development communities in quantum chemistry, currently consisting of over 200 developers spread across a large number of research groups, primarily in academia. For the developers of the code, Q-CHEM is an open team-ware project, where the source code is provided freely, and distributed and updated through a central code repository. The rights of other developers and the company itself are protected through a straightforward non-disclosure agreement that places no restrictions on a developer's ability to publish research describing new theory or algorithms. The activity of the developer community is the key driver behind technical advances in the Q-CHEM software, so that this is very much a symbiotic relationship.

This paper summarises the fourth major release of Q-CHEM, and seeks to accomplish three principal purposes. The first purpose is to review a selection of the technical advances that have occurred in quantum chemistry over the past seven years or so which are incorporated into Q-CHEM 4. The review is, by necessity, relatively non-technical, with a focus on the physical content of the methods and algorithms. We provide brief overviews of the strengths and weaknesses of a large and diverse selection of new methods from the perspective of utility in chemical applications. Complete citations are given to the original literature for readers who are still hungry for further detail. The second purpose is to provide some example case studies of the new methods, particularly those that are not widely used as yet. Such studies provide some specific illustrations of the utility of the methods described in this work for particular chemical applications.

The third purpose of the paper is to serve as the literature citation for release 4 of the Q-CHEM quantum chemistry software package. This purpose is useful because it leads via the technical review to full literature citations for the

key algorithms contained in the program, at the moment in time when this version is current. By contrast, websites are continually updated (and archival material is continually removed), and an author list is an 'empty citation' that does not give the researcher any direct path to further information. The author list of this paper comprises the scientists who have contributed to Q-CHEM in either release 3 or release 4. Authors of earlier versions who have not subsequently contributed may be seen in the reviews describing release 2 [15] and release 3 [17].

The remainder of this paper addresses the challenge of reviewing the science and presenting selected examples under the following organisation. The main areas where methodological advances have been made within our code are reviewed together with a variety of example calculations that illustrate accuracy and/or computational performance, and a selection of chemical case studies. The sequence of topics begins with general purpose electronic structure methods. We treat DFT, which is the most widely used family of electronic structure methods, in Section 2, and discuss recently added functionals for improved accuracy, and algorithmic improvements. Developments in wave function-based methods are reviewed in Section 3. They have the great strength of systematic improvability, particularly at the level of CC theory, where object-oriented design is vital to facilitate development and implementation of new methods. Support for parallel and graphical processing unit (GPU) computing environments is summarised in Section 4, with some example timings.

The standard (and many non-standard) electronic structure methods can be used in a great many ways, starting with recent developments in moving around on the resulting potential energy surfaces, which are discussed in Section 5. We turn next to the problem of treating extended environments in Section 6, which is important for modelling molecules in solution, large clusters, or active sites abstracted from complex systems such as proteins or heterogeneous solids. Energy and electron transfer capabilities are discussed in Section 7, followed by methods for chemical analysis of (at least some classes of) calculations in Section 8. As appropriate for a review of a 'back-end' code, as Q-CHEM fundamentally is, we then finish with a short discussion of the available 'front-ends' that provide input to the back-end, and visualise the resulting output.

Density functional theory

Functionals

Kohn–Sham DFT (KS-DFT)[19] and its extensions provide a foundation for the development of model functionals, but no prescription for how such development should be accomplished. Accordingly, this is an area of great activity.

The full range of density functionals supported in Q-CHEM is too large to comfortably list here, and includes functionals ranging from vintage to brand new. Furthermore, assessing the strengths and weaknesses of different functionals is a major ongoing effort that involves the entire community of both developers and applications specialists. An overview paper cannot summarise this effort, although we can provide a few leading references to comparative studies [20–23] and the main issues [24,25].

We shall discuss some of the new functionals added to Q-CHEM over recent years by considering the current main directions for improved physical content over the predominant density functional for chemistry, which during the last decade was certainly the global hybrid, B3LYP [26].

(1) *Meta-generalised gradient approximation (GGA) and hybrid meta-GGA functionals*: including the kinetic energy density, τ, gives flexibility beyond global hybrids, and therefore is used in many modern density functionals, including M06-L, M06, M06-2X, and M06-HF [27], as well as the recently introduced M11 and M11-L functionals [28,29]. These functionals often yield improved accuracy for thermochemistry (TC) and non-covalent (NC) interactions relative to functionals that do not depend on τ. M06-L and M11-L have the considerable computational advantage of not requiring exact exchange, although there is reduced accuracy, particularly for reaction barrier heights. Other meta-GGA functionals include the constraint-based TPSS [30], as well as its one-parameter hybrid cousin, TPSSh [30].

(2) *Range-separated hybrid functionals*: self-interaction error (SIE), where an electron artificially sees a fraction of itself, is a well-known defect of standard density functionals, and causes artefacts that include spurious delocalisation of unpaired electrons [31,32], and charge-transfer excited states that can be drastically too low [33,34]. While very difficult to remove fully, SIE can be significantly reduced by including 100% exact (wave function) exchange at large electron–electron distances, and a much smaller fraction at short distances, where DFT exchange functionals are effective. Examples of functionals of this type include the LC-ωPBE family of methods [35–38], the ωB97 functionals [39–42], M11 [28], as well as tuned functionals of the BNL type [43,44], where the range-separation parameter can be chosen for the problem at hand based on physical criteria [45,46]. Another option is to include 100% Hartree–Fock (HF) exchange at *all* inter-electronic distances, as in the M06-HF functional [47]. SIE at short inter-electronic distances also affects

TDDFT predictions of core excitation energies and near-edge X-ray absorption fine structure spectra. These short-range SIE errors can be substantially reduced by short-range corrected functionals [48], which are available in Q-Chem.

(3) *Non-covalent interactions*: NC interactions, particularly van der Waals forces, involve non-local correlation effects that are very difficult to treat within a standard correlation functional. Thus, the characteristic R^{-6} long-range interaction potential is absent in traditional local and semi-local density functionals [49]. While it is quite often possible to still obtain an accurate result at the van der Waals minimum without including the long-range R^{-6} behaviour (e.g., with M06-2X or M06-L), several viable methods have emerged that recover the correct long-range behaviour [50]:

- A vast range of dispersion-corrected functionals that include damped C_6/R^6 atom–atom potentials, based on either the Grimme-D2 [51] or -D3 [52] parameterisations are available. Computationally virtually free, but not actually density functionals at all, these methods represent the simplest possible treatment of dispersion.
- Becke's exchange dipole model [53,54] is a novel and accurate method for treating dispersion which has been implemented in Q-Chem in an efficient and numerically stable form [55].
- van der Waals density functionals, which numerically integrate a nonlocal correlation functional that depends simultaneously on $\rho(\mathbf{r})$ and $\rho(\mathbf{r}')$, are a soundly based approach. Examples include vdW-DF-04 [56], vdW-DF-10 [57], VV09 [58], and VV10 [59]. The VV10 form is also used in the very recently developed ωB97X-V functional [42], a 10-parameter semi-empirical functional that is a further evolution of the ωB97 family that reduces the number of empirical parameters, while improving physical content.

(4) *Double hybrid functionals*: based on Görling–Levy perturbation theory as well as semi-empirical considerations, double hybrid functionals (also sometimes called 'doubly hybrid' functionals) include second-order perturbation theory (PT2) corrections to a KS reference. They can yield improved accuracy for both bonded and non-bonded interactions, albeit with increased computational cost and a need for larger basis sets. Q-Chem contains numerous double hybrids, including B2PLYP [60] and B2PLYP-D [61], XYG3 [62], ωB97X-2 [41], and PBE0-2 [63]. XYGJ-OS is an opposite spin double hybrid [64], which scales as only $O(M^4)$,

for which the analytical gradient is also available [65].

(5) *Becke post-self-consistent field (SCF) functionals*: the semi-empirical B05 post-SCF functional [66,67] uses the Becke–Roussel exchange model [68] to compute a local analogue to the exact exchange hole. The extent of delocalisation of the exact exchange hole is used as a parameter for capturing both same-spin and opposite-spin non-dynamical correlation within a single determinant framework. Coupled with the modified Bc88 correlation functional (BR94) [69,70] to capture dynamical correlation, the performance of the six-parameter B05 functional parallels the performance of existing hybrid meta-GGA functionals for atomisation energies and barrier heights. A self-consistent version of the B05 functional has been efficiently implemented [71] into Q-Chem 4, including a resolution-of-the-identity (RI) version that greatly reduces the cost of computing the exact exchange energy density [72].

To provide just a glimpse of the comparative performance of some of the standard functionals available in Q-Chem, Table 1 shows the root mean square (RMS) errors associated with a variety of density functionals on some established test sets for bonded and non-bonded interactions. Of the 10 data-sets, the first 4 (TAE, Alk19, DBH24, and G21IP) correspond to TC datapoints (203 total), while the latter 6 (HW30, S22, S66, A24, X40, and DS14) correspond to NC interaction datapoints (196 total). Computational details and specific data-set information can be found in [42]; comparisons of GGA functionals trained on the same data with different choices of non-local exchange and correlation have also been presented recently [73].

For the bonded interactions, it is clear that exact exchange is very useful, as the two best functionals are the range-separated hybrid GGA ωB97X-V functional and the global hybrid meta-GGA M06-2X functional, with RMS errors around 3 kcal/mol. In comparison, the best local functional for TC (M06-L) has an RMS error that is nearly double that of the best hybrid functional. For non-bonded interactions, the range-separated hybrid GGA ωB97X-V functional outperforms the next best density functional by almost a factor of 2. However, local meta-GGA functionals like M06-L can compete with well-established dispersion-corrected hybrid functionals such as ωB97X-D. On the popular S22 data-set, the three best density functionals are ωB97X-V, ωB97X-D, and M06-L, with RMS errors of 0.23, 0.41, and 0.43 kcal/mol, respectively. For a more comprehensive assessment of these density functionals on a data-set of over 2400 datapoints, the reader is referred to Table 6 in [42].

Table 1. RMS errors in kcal/mol for 17 density functionals available in Q-CHEM on 10 data-sets comprising 399 datapoints. The first four data-sets contain bonded interactions, representative of thermochemistry (TC), evaluated using the aug-cc-pVQZ basis. The latter six data-sets contain non-covalent (NC) interactions, which are evaluated using the aug-cc-pVTZ basis, except for the X40 data, which used the def2-TZVPPD basis set. The TC data-sets are (1) non-multi-reference total atomisation energies (TAE) [74], (2) atomisation energies of $n = 1$–8 alkanes (Alk19) [75], (3) diverse barrier heights (DBH24) [76–78], (4) adiabatic ionisation potentials (G21IP) [79,80], (5) weak hydrocarbon–water interactions (HW30) [81], (6) hydrogen-bonded and dispersion-bonded complexes (S22) [82,83], (7) interaction energies of relevant biomolecular structures (S66) [84,85], (8) small non-covalent complexes (A24) [86], (9) non-covalent interactions of halogenated molecules (X40) [87], and (10) interactions of complexes containing divalent sulphur (DS14) [88]. The final two columns give the overall RMS errors for the four TC data-sets and six NC data-sets.

	#	TAE 124	Alk19 19	DBH24 24	G21IP 36	HW30 30	S22 22	S66 66	A24 24	X40 40	DS14 14	TC 203	NC 196
PBE-D2	1	16.94	26.21	10.37	4.81	0.71	0.70	0.63	0.59	0.74	0.57	16.01	0.67
PBE-D3	2	16.85	20.93	10.27	4.81	0.48	0.60	0.46	0.41	0.59	0.47	15.20	0.50
B3LYP-D2	4	5.28	0.64	5.28	4.86	0.53	0.74	0.62	0.39	0.47	0.28	4.95	0.55
B3LYP-D3	5	5.23	5.50	5.23	4.86	0.35	0.50	0.43	0.23	0.34	0.23	5.19	0.38
B3LYP-NL	4	5.92	14.74	6.01	4.35	0.21	0.68	0.46	0.27	0.43	0.24	7.03	0.43
B97-D2	11	4.06	9.28	4.36	3.48	0.35	0.60	0.36	0.26	0.43	0.25	4.74	0.39
B97-D	9	5.18	10.48	7.18	4.47	0.40	0.54	0.52	0.32	0.59	0.37	6.03	0.49
VV10	2	12.46	5.85	9.86	5.43	0.43	0.63	0.52	0.41	0.63	0.52	10.71	0.53
LC-VV10	3	5.30	19.04	3.02	5.23	0.30	0.51	0.31	0.15	0.41	0.12	7.55	0.34
ωB97X	14	3.50	2.84	2.33	3.79	0.45	0.95	0.50	0.40	0.54	0.36	3.38	0.55
ωB97X-D	15	3.65	2.90	2.07	3.82	0.35	0.41	0.52	0.15	0.49	0.18	3.47	0.43
ωB97X-V	10	3.34	0.71	1.81	3.57	0.20	0.23	0.18	0.09	0.21	0.05	3.09	0.18
M06-L	34	5.54	8.11	5.38	5.60	0.35	0.43	0.36	0.23	0.48	0.25	5.82	0.38
M06	33	3.94	4.63	2.97	3.78	0.33	0.77	0.53	0.25	0.57	0.34	3.88	0.51
M06-2X	29	3.24	5.27	1.12	3.49	0.46	0.47	0.29	0.28	0.28	0.20	3.37	0.34
M11-L	44	6.62	29.35	3.54	4.54	0.48	0.91	0.81	0.46	1.23	0.59	10.61	0.84
M11	40	4.37	3.94	1.48	4.64	0.38	0.58	0.41	0.27	0.54	0.30	4.15	0.44

2.2. *Electric and magnetic molecular properties*

The calculation of molecular properties provides an important link to experiment and many linear-scaling methods have been developed over recent years that allow to compute molecular systems with more than 1000 atoms (see, e.g., [89–92]). The Q-CHEM program package allows the computation of a wide range of properties at the HF and KS-DFT levels. Apart from determining geometries, vibrational spectra, and electronic excitations, the new version of Q-CHEM offers several new and improved efficient linear-scaling methods to evaluate different electric and magnetic response properties for large systems. These range from the calculation of NMR chemical shieldings using density matrix-based coupled-perturbed SCF theory [93,94] (also for large basis sets with up to g functions in the new version) to electric response properties [95,96] by an implementation of the density matrix-based time-dependent SCF algorithm [97] that allows for calculating static and dynamic polarisabilities and first hyperpolarisabilities. Here, an overall asymptotic linear-scaling behaviour can be reached by employing $\mathcal{O}(N)$ integral evaluations based on CFMM [98] and LinK [99,100] in combination with efficient sparse algebra routines [93].

Furthermore, the combination of linear-scaling QM methods for calculating molecular properties with simple molecular mechanics (MM) schemes (QM/MM) has proven to be a very valuable tool for studying complex molecular systems. The linear-scaling methods allow to systematically converge the property with the chosen QM sphere, and convergence for QM/MM schemes is typically clearly faster than in pure QM calculations, since in complex systems long-range electrostatics are accounted for (see, e.g., [92,101,102]).

As another new feature, the calculation of indirect nuclear spin–spin coupling constants (*J*-coupling) [103,104] is introduced. The implementation uses the LinK scheme [99,100] for the construction of exchange-type matrices for non-metallic systems. A fully density matrix-based algorithm is currently in development [105]. Basis functions with angular momenta up to g are supported. Predictions of good accuracy for *J*-couplings can be obtained [106,107] especially when using specialised basis sets [108–111], several of which have been added to the basis set library.

The *J*-based configurational analysis [112] is a robust technique for the structural elucidation of even large organic molecules [113]. In the past, analyses of *J*-couplings have mostly utilised the Karplus equations [114–116], which relate ^3J-coupling constants to the dihedral angle between atoms. Moving from empirical equations to predictions from first principles, for example with DFT, is desirable

not only because the predictions are expected to be more reliable, but also because it expands their applicability. Long-range *J*-couplings [117], or even couplings through hydrogen bonds [118], neither of which are tractable with current empirical methods, can naturally be studied by computational chemistry if an adequate level of electronic structure theory is selected.

2.3. *Algorithm developments*

A great variety of algorithmic improvements for DFT calculations have been incorporated into Q-CHEM. Those to do with parallel computing are covered separately in Section 4.

Resolution-of-the-identity methods: for large atomic orbital (AO) basis sets in particular, RI methods offer substantially improved performance relative to exact evaluation of two-electron integrals with nearly negligible loss of accuracy, if appropriately optimised auxiliary basis sets are employed. The Karlsruhe group associated with TurboMole has been amongst the leading developers of such basis sets. The standard RI method may be further enhanced by performing local fitting of a density or function pair element. This is the basis of the atomic-RI method (ARI), which has been developed for both Coulomb (*J*) matrix [119] and exchange (*K*) matrix evaluation [120]. In ARI, only nearby auxiliary functions $K(r)$ are employed to fit the target function. This reduces the asymptotic scaling of the matrix-inversion step as well as that of many intermediate steps in the digestion of RI integrals. Briefly, atom-centred auxiliary functions on nearby atoms are only used if they are within the outer radius (R_1) of the fitting region. Between R_1 and the inner radius (R_0), the amplitude of interacting auxiliary functions is smoothed by a function that goes from zero to one and has continuous derivatives. To optimise efficiency, the van der Waals radius of the atom is included in the cutoff so that smaller atoms are dropped from the fitting radius sooner. Energies and gradients are available.

Multi-resolution exchange-correlation (MrXC) quadrature: MrXC [121–123] can accelerate the numerical quadrature associated with computation of the XC energy and the XC matrix needed in the SCF procedure. It is an algorithm for seamlessly combining the standard atom-centred grid of quantum chemistry, with a cubic grid of uniform spacing by placing the calculation of the smooth part of the density and XC matrix onto the uniform grid. The computation associated with the smooth fraction of the electron density is the major bottleneck of the XC part of a DFT calculation and can be done at a much faster rate on the cubic grid due to its low resolution. Fast Fourier transform and B-spline interpolation are employed for the accurate transformation between the two types of grids such that the final results remain the same as they would be on the atom-centred grid alone. By this means, a speedup of several times for the calculations of the XC matrix is achieved. The smooth part of

the calculation with MrXC can also be combined with the Fourier transform Coulomb method [124] to achieve even higher efficiency, particularly for calculations using large basis sets and diffuse functions.

TDDFT gradients and Hessians: a recent implementation of TDDFT analytical gradients (also in the Tamm–Dancoff approximation [125]) is available [126], with parallel capabilities. A more distinctive capability is the availability of an implementation of TDDFT analytical frequencies (greatly extending an existing analytical configuration interaction with single substitutions [CIS] frequency code [127]), both in the Tamm–Dancoff approximation [128] and for full TDDFT [129]. In addition, analytical TDDFT gradients and frequencies have been extended [130] to include the smooth polarisable continuum models for solvation that are discussed in Section 6.1. Compared to numerical differentiation, analytical second derivatives of the excitation energy yield higher precision and need much less computer time, but require much more memory. The memory usage is mainly dominated by the geometric derivatives of the MO coefficients and transition amplitudes, which is dealt with by solving the coupled-perturbed equations in segments. To ensure high precision, a fine grid for numerical integration should be used, since up to fourth-order functional derivatives with respect to the density variables as well as their derivatives with respect to the nuclear coordinates are needed.

Dual basis methods: an effective method for reducing the computational cost of SCF calculations is to perform the SCF calculation in a small ('primary') basis set, and subsequently correct that result in a larger ('secondary') basis set, using perturbation theory. Q-CHEM contains two related approaches for performing dual basis calculations. Both energies and analytical gradients are available for the dual basis approach of Head-Gordon and co-workers [131,132], who have also developed dual basis pairings for the Dunning cc-pVXZ [133] and aug-cc-pVXZ [134] basis sets. From a good reference, the HF perturbation theory approach [135,136] provides more accurate corrections even at first order, and is also applicable to DFT calculations. Not only jumps in basis set, but also in the choice of quadrature grid, and density functional itself are possible via the 'triple jumping' approach [137].

Metadynamics and non-orthogonal configuration interaction (NOCI): SCF metadynamics [138] allows one to find alternative minima within the SCF framework (either HF or KS-DFT). Alternative minima are obtained by applying a bias in density matrix space at the locations of previously found minima and using standard convergence algorithms on this modified potential energy surface. It is then possible to perform NOCI [139,140] using the resulting non-orthogonal determinants as a basis. One then builds and diagonalises the Hamiltonian in this representation. Q-CHEM supports the use of general and complex HF orbitals for this purpose. While calculation of the
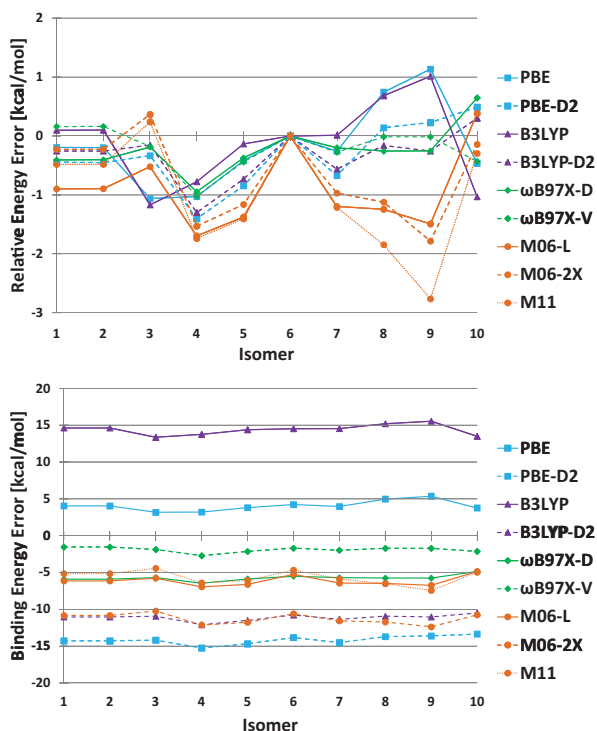
Figure 1.   Relative and binding energy errors for 10 isomers of $F^-(H_2O)_{10}$ with respect to RI-CCSD(T)/CBS benchmark values.

Hamiltonian is more complicated than in orthogonal CI, it has been shown for some systems that the number of determinants to obtain qualitatively accurate results for ground and excited states of challenging systems such as polyenes is rather small (less than 100 or so) [140].

2.4.   Case study: relative and binding energies of 10 $F^-(H_2O)_{10}$ isomers

In a recent paper [141], Herbert and co-workers discovered that halide–water clusters present a challenge for density functionals such as LC-VV10, ωB97X-D, and M06-2X. In particular, the binding energies of 10 isomers of $F^-(H_2O)_{10}$ proved to be the most notorious case. Using the same geometries and reference values, nine density functionals available in Q-CHEM were benchmarked on these 10 isomers, and the results, calculated in the aug-cc-pVTZ basis set with a (99,590) grid, are provided in Table 2 and Figure 1. Table 2 confirms that a majority of these
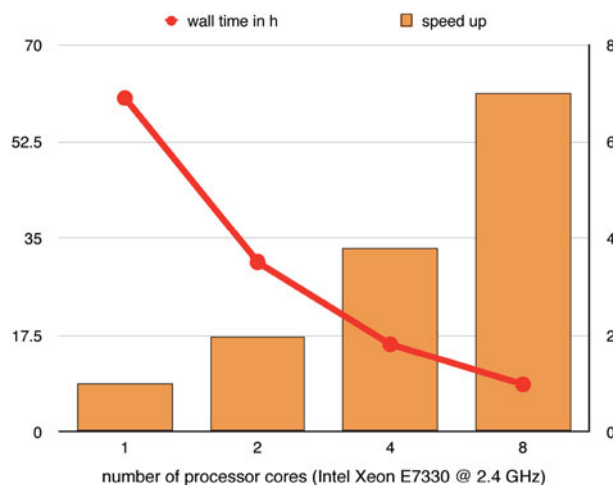

Figure 2.   Timings and parallel speedup of an ADC(3) calculation of the benzene molecule using aug-cc-pVTZ basis set.

density functionals are unable to accurately predict the binding energies of these isomers. However, the newly developed ωB97X-V functional performs at least two times better than the next best functional, which is (surprisingly) PBE. In order to identify if the functionals in question are underbinding or overbinding the clusters, it is useful to consider Figure 1. Besides PBE and B3LYP, all of the density functionals overbind the isomers, with B3LYP-D2, M06-2X, and PBE-D2 overbinding more severely than the rest. ωB97X-D, M06-L, and M11 overbind considerably as well, though by approximately 5 kcal/mol instead of more than 10 kcal/mol. For the relative energies of the clusters, the Minnesota functionals perform poorly, with errors larger than 1 kcal/mol. The two best functionals are ωB97X-V and ωB97X-D, with RMS errors of 0.40 and 0.45 kcal/mol, respectively. The parallel performance of ADC(3) calculations on the benzene molecule is illustrated in Figure 2.

3.   Wave function methods

3.1.   Perturbative methods

Second-order Møller–Plesset perturbation theory [142,143] is widely used as the simplest and most computationally inexpensive wave function treatment of dynamic correlation. Q-CHEM's workhorse implementation based on RI algorithms for the energy and gradient [144,145] is

Table 2.   Relative and binding energy RMS errors in kcal/mol for 10 isomers of $F^-(H_2O)_{10}$ with respect to RI-CCSD(T)/CBS benchmark values.

RMSD	PBE	PBE-D2	B3LYP	B3LYP-D2	ωB97X-D	ωB97X-V	M06-L	M06-2X	M11
Relative energy	0.68	0.63	0.68	0.54	0.45	0.40	1.10	0.97	1.35
Binding energy	4.11	14.19	14.42	11.13	5.76	1.94	6.17	11.30	5.74

Table 3. CPU times on a single CPU core and scaling behaviour for conventional RI-MP2 as well as RI-CDD-MP2 calculations on model DNA systems in a def2-SVP basis. The index of the DNA systems denotes the number of A–T base pairs. For full details and additional performance data can be found in [148].

	# Basis	RI-MP2		RI-CDD-MP2	
System	Functions	Time (h)	Scaling	Time (h)	Scaling
DNA$_1$	625	0.16	–	0.23	–
DNA$_2$	1332	6.36	4.87	4.75	4.02
DNA$_4$	2746	231.63	4.97	53.22	3.34
DNA$_8$	5574	–	–	449.53	3.01

highly efficient for small- and medium-size molecules. For greater efficiency in larger basis sets, energies [133] and gradients [146] are also available for the dual basis RI-MP2 method. For larger molecules, an efficient cubic-scaling MP2 method has been implemented in Q-CHEM. The method is grounded on the atomic orbital-based MP2 formulation and uses a Cholesky decomposition of pseudo-density matrices (CDD) [147,148] in combination with integral screening procedures using QQR integral estimates [148–150]. Using the RI approach and efficient sparse matrix algebra, the RI-CDD-MP2 method shows a fairly small prefactor for a reduced-scaling method. Due to the asymptotically cubic scaling of the computational cost of the RI-CDD-MP2 method with the size of the molecule, the approach is faster for larger systems than the conventional fifth-order scaling RI-MP2 method. The crossover between RI-CDD-MP2 and conventional RI-MP2 is found already for systems as small as, e.g., two DNA base pairs as shown by the timings in Table 3.

While MP2 greatly improves on the mean-field reference in many cases, it also has some well-known weaknesses. These include a need for large basis sets, overestimation of intermolecular interactions, and susceptibility

to spin-contamination. Q-CHEM contains a variety of recently developed methods that partially lift some of these limitations. For ground state treatment of intermolecular interactions, Q-CHEM contains newly developed attenuated MP2 methods, which offer remarkable improvements in accuracy for small- and medium-sized basis sets. Attenuated MP2 [151–153] is available with the Dunning aug-cc-pVDZ (small) and aug-cc-pVTZ (medium) basis sets. This approach works by cancelling the overestimation of intermolecular interactions by attenuation of the long-range part of the correlation energy. A summary of the RMS errors (kcal/mol) obtained for a series of inter- and intramolecular non-bonded interactions is given in Table 4. Consistent improvement relative to unattenuated MP2 is found for databases of hydrogen-bonded, dispersion, and mixed interactions (divalent sulphur, A24, S22, S66, and L7). Relative conformational energies for sulphate–water clusters, alkane conformers (ACONF), cysteine conformers (CYCONF), sugar conformers (SCONF), and dipeptide and tripeptide conformers (P76) are in good agreement with benchmarks.

As a further evolution of spin-component scaled MP2 methods for systems susceptible to spin-contamination,

Table 4. Root mean squared errors (in kcal/mol) for databases of non-bonded interactions, grouped by intermolecular or intramolecular interactions. Only equilibrium geometries were examined from the divalent sulphur database [154]. Complete basis set estimates (CBS) for MP2 were taken from references for the divalent sulphur, SW49 [155–157], ACONF [158], CYCONF [159], and SCONF [160] databases. MP2/CBS results for the S22 [82,83], S66 [84,85], L7 [161], and P76 [162] databases were obtained from the Benchmark Energy and Geometry DataBase (BEGDB) [163]. MP2/CBS results for the A24 databases [164] were generated for this work.

	MP2/aDZ	MP2(terfc, aDZ)	MP2/aTZ	MP2(terfc, aTZ)	MP2/CBS
Divalent sulphur	1.25	0.28	0.80	0.16	0.41
A24	0.52	0.26	0.31	0.18	0.21
S22	3.91	0.61	2.5	0.48	1.39
S66	2.66	0.43	1.53	0.25	0.73
L7	24.14	1.10	14.00	1.87	8.78
SW49(bind)	1.23	1.03	0.84	0.36	0.34
SW49(rel)	0.49	0.34	0.34	0.39	0.10
ACONF	0.31	0.29	0.24	0.08	0.11
CYCONF	0.20	0.28	0.30	0.21	0.25
SCONF	0.28	0.52	0.22	0.12	0.21
P76	1.06	0.33	0.59	0.31	0.42

the orbital optimised opposite spin (O2) method is available (energies [165] and gradients [166]). Relative to full OO-MP2, which exhibits systematic overbinding, O2 yields higher accuracy by virtue of its single semi-empirical scaling parameter, and also lower computational cost ($O(M^4)$ vs. $O(M^5)$) by virtue of containing no same-spin contribution [167]. In addition to cleaning up spin-contamination problems [165], O2 also avoids the n-representability and force discontinuity issues of MP2 [168]. At higher computational cost than O2 (same cost as OO-MP2), the recently introduced δ-OO-MP2 method [169] simultaneously solves the problems of overestimating correlation effects and divergences from vanishing denominators in small-gap systems by using a regularisation, or level shift, parameter.

Beyond ground states, the corresponding second-order correction to single excitation CI for excited states [170], CIS(D), offers similar advantages to MP2 and suffers from very similar limitations. Within Q-CHEM, more computationally efficient excited state scaled opposite-spin methods are available, that, like SOS-MP2 and O2, scale as $O(M^4)$. SOS-CIS(D), a non-degenerate method [171], is available for excited state energies. SOS-CIS(D0), a quasi-degenerate approach, which is therefore more robust at the cost of some additional computation, has both energies [173] and analytic gradients [174,175] available.

3.2. Coupled cluster methods

Q-CHEM 4 features a wide variety of computational methods for the ground and excited states based on CC theory [176,177]. These methods are amongst the most versatile and accurate electronic structure approaches. The equation-of-motion (EOM) approach extends single-reference CC methods to various multi-configurational wave functions. Q-CHEM 4 includes EOM-CC methods for electronically excited states (EOM-EE), ionised/electron-attached ones (EOM-IP/EA), as well as doubly ionised (EOM-DIP) [178] and spin-flip (EOM-SF and EOM-2SF) [179,180] extensions that enable robust and reliable treatment of bond-breaking, diradicals/triradicals, and other selected multi-configurational wave functions. Gradient and properties calculations (including interstate properties) are available for most CC/EOM-CC methods.

Q-CHEM 4 offers an efficient multi-core parallel implementation of these methods based on a general purpose tensor library [181]. The library provides a convenient tensor expressions C++ interface that aids new developments.

In order to reduce computational requirement for the CC methods and improve parallel performance, we exploited two reduced-rank approaches based on RI and Cholesky decomposition (CD) of two-electron repulsion integrals [172]. The equations were rewritten to eliminate the storage of the largest four-dimensional intermediates leading to a significant reduction in disk storage requirements, reduced I/O penalties, and, as a result, improved parallel performance.

Table 5. Timings of one CD-CCSD iteration (in hours) for $(mU)_2$-H_2O (test 4 in [172]) using 1E-2 threshold for Cholesky decomposition. This calculation takes 12 CCSD iterations to converge.

Method	Basis	# Basis functions	Memory limit	Wall time
CD-CCSD	6-31+G(d,p)	489	100 GB	5.1
CD-CCSD/FNO	6-31+G(d,p)	489	100 GB	1.4
cc-pVTZ/FNO	cc-pVTZ	882	300 GB	12.2

For medium-size examples, RI/CD calculations are approximately 40%–50% faster compared with the canonical implementation. More significant speedups (two- to five-fold) are obtained in larger basis sets, e.g., cc-pVTZ.

Even more considerable speedups (six- to seven-fold) are achieved by combining RI/CD with the frozen natural orbitals approach [182]. Importantly, with Q-CHEM, one can perform CC/EOM-CC calculations for relatively large systems (up to $\sim$1000 basis functions) on mainstream single-node servers. Detailed performance benchmarks are available in [172,181]. Table 5 shows selected timings obtained on a single 16-core Xeon-Dell node for dimethyl-uracyl dimer solvated by one water molecule ($(mU)_2$-H_2O, C1 symmetry, 158 electrons). Frozen natural orbital (FNO) calculations in Table 5 used an occupation threshold of 99.5%. As an example, for the 6-31+G(d,p) basis, this corresponds to 292 active virtual orbitals and 118 frozen virtuals. Using FNO leads to errors in IEs that are less than 0.02 eV relative to the full calculation, which is typical for this threshold [182].

While conventional CC and EOM methods allow one to tackle electronic structure ranging from well-behaved closed-shell molecules to various open-shell and electronically excited species [177], metastable electronic states, so-called resonances, present a difficult case for theory. By using complex scaling and complex absorbing potential techniques, we extended these powerful methods to describe autoionising states, such as transient anions, highly excited electronic states, and core-ionised species [183–185]. In addition, users can employ stabilisation techniques using charged sphere and scaled atomic charges options [186]. Various improvements of iterative diagonalisation algorithms enable access to high-lying interior eigenvalues.

3.3. Algebraic diagrammatic construction (ADC) methods

Algebraic diagrammatic construction (ADC) methods constitute a series of methods for the calculation of excited states which derive from the perturbation expansion of the polarisation propagator [187,188]. Each method differs in the approximation to the Hamiltonian matrix for which the eigenvalue problem has to be solved, as well

as in the way state properties and transition properties are computed from the eigenvectors. In first order, the ADC(1) eigenvalue problem is identical to CIS, but additional terms enter in the computation of transition moments. The second-order approximation, ADC(2) provides excitation energies (and transition properties) comparable to those obtained with CIS(D) [170] and CC2 [189,190]. An extension to the second-order scheme ADC(2)-x adds additional terms to the Hamiltonian matrix which put more weight on doubly excited configurations. As a result, the excitation energies are shifted to lower energies, in particular if the respective states possess strong double excitation character. Accordingly, the comparison of ADC(2)-x and ADC(2) results can yield useful insights about the importance of double excitations in the spectrum [191]. With the third-order method, ADC(3) the accuracy of the excitation energies improves further, getting close to the results obtained by CC3 calculations, though at computational costs which are an order of magnitude smaller.

In Q-CHEM, ADC methods up to third order are available for the computation of excited states [192]. They have been implemented based on the same general purpose tensor library [181] as the CC methods, offering shared-memory parallelisation and a LaTeX style programming interface for new equations. The implementation allows for the calculation of excitation energies and transition properties from the ground state, as usual. In addition, excited state properties and transition properties between excited states can be computed on request. From those, two-photon absorption cross-sections can be deduced via sum-over-states expressions. Alternatively, the two-photon absorption cross-section can be obtained by inversion of the ADC matrix [193]. For visualisation of the excited states, transition densities or attachment and detachment densities may be exported as grid data for later display by standard visualisation tools.

Furthermore, Q-CHEM features spin-opposite scaled (SOS) ADC variants for both second-order schemes ADC(2) and ADC(2)-x [194]. They follow the idea of SOS-MP2 to reduce computational costs and improve the resulting energies. Therefore, same-spin contributions in the ADC matrix are neglected, while opposite-spin contributions are scaled using appropriate semi-empirical parameters. SOS-ADC(2) requires two scaling parameters c_{os} and c_c, while for SOS-ADC(2)-x another parameter c_x is needed. The parameter $c_{os} = 1.3$ is inherited from SOS-MP2 for the scaling of the T_2 amplitudes, while the parameters c_c and c_x are used to scale the ph/2p2h block and the off-diagonal part of the 2p2h/2p2h block of the ADC matrix, respectively. For SOS-ADC(2) the optimal value of $c_c = 1.17$ was determined by fitting against the Thiel benchmark set [195]. A similar fit for SOS-ADC(2)-x yielded $c_c = 1.0$ and $c_x = 0.9$ as optimal values [194]. With these parameters, a mean absolute error of 0.14 eV in the excitation energies is achieved by SOS-ADC(2) for the Thiel benchmark set. For SOS-ADC(2)-x, the mean absolute

error for predominantly single excitations becomes 0.17 eV, while for states with large double excitation character, it is 0.21 eV.

Another set of ADC variants in Q-CHEM uses the core–valence separation (CVS) approximation [196] to calculate core excitations. In general, the calculation of core-excited states is quite difficult, since with standard implementations the valence excited states need to be calculated before any core-excited state can be obtained. The CVS approximation solves this problem by decoupling core and valence excitations in the ADC Hamiltonian. Thereby, it makes use of the fact that the interactions between core and valence excitations are negligible due to the strong localisation of the core orbitals and the large energy separation between core and valence orbitals. As result, core-excited states can be computed independently from the core-excitation part of the ADC Hamiltonian, which significantly reduces the computational costs compared to the calculation of valence-excited states. CVS variants for ADC(1), ADC(2), and ADC(2)-x are available with CVS-ADC(2)-x showing excellent agreement with experimental data [197].

3.4. Density matrix renormalisation group

Q-CHEM now includes an interface to the density matrix renormalisation group (DMRG) code of Sharma and Chan ('Block') [198–201]. The DMRG [198–211] is a variational wave function method based on a class of wave functions known as matrix product states (MPS) [208,212]. The DMRG allows for unique kinds of quantum chemical calculations to be performed. The accuracy of the DMRG can be continuously tuned based on a single parameter, the number of renormalised states, denoted M. In typical calculations, M ranges from 1000 to 10,000. By increasing M, it is possible to push DMRG calculations to yield highly accurate energies (e.g., to within 10–100 microHartrees of the exact result) for systems much larger than can be treated with full configuration interaction (FCI) [213–215]. While convergence with M is system dependent, as a guide, for a modest number of electrons (10–20), high accuracy can be achieved for more than 100 orbitals, while for larger number of electrons (e.g., up to 40), high accuracy can be achieved for about 40 orbitals, using M up to 10,000.

Furthermore, because the MPS is not built on an excitation expansion around a Slater determinant, DMRG calculations are well suited to describe *strong* or *multi-reference* correlation, as found in transition metals or excited states [208]. Here, the DMRG is often used to replace a complete active space calculation [205,216,217]. Active spaces with up to 40 orbitals can be treated reliably, and the DMRG has been applied to bioinorganic complexes with as many as four transition metal ions, such as the Mn_4Ca cluster of photosystem II [218], and [4Fe-4S] clusters. Finally, the MPS mathematically represents one-dimensional chain-like correlations very efficiently. The DMRG can thus be used with

great effect in treating correlations in π-systems of many conjugated molecules [216,219,220].

The version of Block included with Q-CHEM can be run in an entirely black-box fashion; orbital ordering, one of the more unusual inputs into a DMRG calculation, can be determined automatically using a graph-theoretical algorithm, or a genetic algorithm optimisation. The user need only specify the final number of states (*M*) desired. The DMRG module is also completely parallelised; larger calculations as described above should be run on 10–100 cores.

3.5. *Active space spin-flip methods*

This is a family of methods capable of treating strong correlations via an active space at lower computational cost than complete active space SCF (CASSCF) type methods, and with greater ease of use. A molecule with strong correlations requires multi-configurational wave functions to be even qualitatively correct. For two strongly correlated electrons, the first such approach is the spin-flip extended single configuration interaction (SF-XCIS) model [221]. For general numbers of strongly correlated electrons (though computational cost increases exponentially with the number of spin-flips), two implementations [222,223] of the restricted active space spin-flip (RAS-SF) model [224,225] are available. These methods start from a high spin restricted open-shell HF determinant, where the strongly correlated electrons are initially all high spin. The target low-spin strongly correlated states are accessed by flipping the spins of half the high spin levels (which define the active space), and performing a full CI calculation in the active space, augmented by single excitations into and out of the active space. These additional 'particle' (p) and 'hole' (h) excitations provide state-specific relaxation of the orbitals.

The efficient implementation of the RAS-SF (i.e., spin-flipping in the RAS-CI formalism) has enabled detailed electronic structure studies of singlet fission in dimers plus environment models of pentacene and tetracene crystals [226–229]. Relevant electronic states include delocalised excitonic states, with a variable admixture of charge-resonance configurations, interacting with a dark multi-exciton state of a doubly excited character. Importantly, the RAS-2SF method allows one to treat all electronic states within the same computational framework in dimers and even trimers of relevant compounds (tetracene, pentacene, hexacene, etc). RAS-SF calculations enabled investigations of the effect of morphology on the state couplings.

Very recently, the efficiency of the methods has been increased by treating the excitations into and out of the active space perturbatively, to define the SF-CAS(h,p) method [230]. The basic idea is that if the states of interest are predominantly described by active space configurations, then the small state-specific relaxations that are accounted for by the particle and hole excitations in RAS-SF can be accurately approximated by perturbation theory at much lower
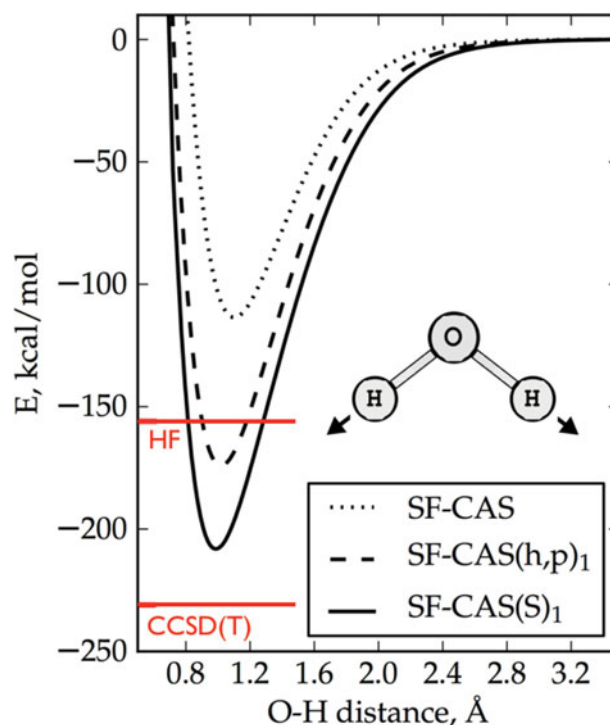

Figure 3. H_2O potential energy surfaces for double dissociation in the aug-cc-pVTZ basis set. SF-CAS is the dotted line, SF-CAS(h,p)$_1$ is the dashed line, and SF-CAS(S)$_1$ is the solid line. The upper red line is the HF binding energy (no correlation), and the lower red line is the CCSD(T) binding energy (nearly complete treatment of correlation effects at equilibrium vs. dissociation).

computational cost. The perturbative framework also permits treatment of extended single excitations that go from the hole space to the particle space (i.e., 'hole–particle' excitations), as the active space is rearranged, defining the SF-CAS(S) method [231]. SF-CAS(S) is a method that contains physics that goes beyond RAS-SF, and therefore begins to account for effects that we would normally identify as being associated with dynamic correlation.

As an example of the performance of the newest SF-CAS methods, one may consider the simultaneous bond dissociation of H_2O. In the aug-cc-pVTZ basis set, CCSD(T) provides a binding energy of 231 kcal/mol, with 75 kcal/mol attributed to dynamical electron correlation. In Figure 3, the computed bond dissociation curves for the SF-CAS, SF-CAS(h,p)$_1$, and SF-CAS(S)$_1$ methods are compared. In general, a single spin-flip takes care of a single bond dissociation. In this example, two bonds are broken, requiring two spin-flips from the quintet restricted open shell Hartree–Fock (ROHF) reference.

While all the methods smoothly dissociate to correct products without spin-contamination, the binding energy for SF-CAS is significantly less than even that of unrestricted HF (UHF), reflecting the biasing of quintet orbitals against the bound singlet state. The perturbative treatment

of hole and particle states in SF-CAS(h,p)$_1$ improves this binding (-174 kcal/mol) to a value that is slightly better than the uncorrelated UHF method, while avoiding any spin-contamination or kinks in the PES. Adding the full singles correction perturbatively, SF-CAS(S)$_1$ significantly increases the binding, to 208 kcal/mol, which corresponds to recovering a considerable fraction of the dynamical correlation energy.

3.6. Coupled cluster valence bond

The perfect pairing (PP) approximation [232,233] treats a molecular system as a collection of semi-independent electron pairs. In fact, this treatment is quite compatible with the classic Lewis dot structure picture of bonds and lone pairs. When neighbouring covalent bonds are broken, resulting in open-shell fragments, they can become strongly coupled to each other, invalidating the semi-independence assigned to them by PP. This is true for double and triple bonds, for example, and in such cases the PP energy will lie far above the sum of the energies of the dissociated fragments. The coupled cluster valence bond (CCVB) approximation [234] was introduced to account for this strong coupling, while retaining the simple Lewis picture of PP. CCVB possesses exact spin symmetry, will give correct energy profiles in these sorts of bond dissociations, and incurs only a modest computational cost (the number of variables describing the strong correlations between pairs smaller than the number of MO coefficients). CCVB can treat both open- and closed-shell systems. CCVB is particularly useful for the lowest energy state of each spin multiplicity for systems with strong spin correlations, such as the example discussed below. The main limitation of CCVB is that, effectively, it models only one Lewis dot structure at a time, and this can result in irregularities in situations where resonance effects are significant, as discussed in more detail elsewhere [235].

As an example of the application of CCVB, we have computed the potential energy surface for the dissociation of Cr_2. The Cr_2 molecule has a formal hextuple bond, amounting to six strongly correlated electron pairs, and it is well recognised as a difficult multi-reference problem in which static and dynamic correlation effects are both important [236]. The canonical multi-reference approach for Cr_2 is to employ a 12 electrons in 12 orbitals complete active space, which entails many thousands of configurations (the naive number is $\left(^{12}C_6\right)^2$). In contrast, the CCVB wave function for this case is built from only 21 parameters. We have included CASSCF and UHF results, and all calculations used the Wachters+f basis set [237–239]. The energies are relative to two times the septet-spin Cr energy.

The results of our calculations are given in Figure 4. The principal purpose is to illustrate the ability of CCVB to capture the important static correlations associated with bond-breaking in this system. Such correlations are so important
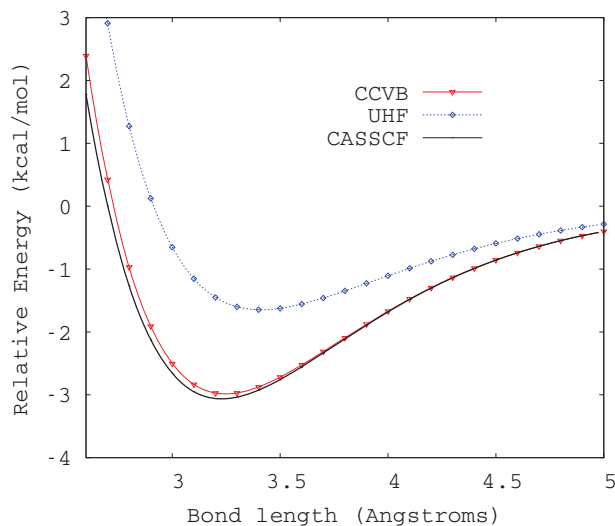

Figure 4. A plot of the potential curve for Cr_2 molecule, treated by the CASSCF method using 12 electrons in 12 orbitals, by CCVB correlating six electron pairs, and by the spin-polarised UHF method. The difference between UHF and CASSCF can be viewed as defining the strength of static correlations in this molecule.

that the UHF wave function is spin-polarised at all bond lengths shown: the restricted solution is not stable anywhere in the range shown! For static correlation, CASSCF represents the exact solution of the (12,12) Schrödinger equation, and is the benchmark against which CCVB can be tested. Across the range of bond lengths shown, CCVB is remarkably close to CASSCF, while UHF, with its spin contamination error, is clearly inferior. Furthermore, the optimal bond lengths are 3.23, 3.25, and 3.41 Å, for CASSCF, CCVB, and UHF, respectively. Finally it should be remembered that the experimentally derived equilibrium bond length of Cr_2 is only 1.7 Å, and the binding energy is about 35 kcal/mol, which indicates the key role of dynamic correlation, which is not considered in CCVB (or CASSCF).

4. Advanced computing capabilities

Shared memory parallel routines for DFT and HF energies and gradients have been recently implemented in Q-CHEM by Zhengting Gan. The key computational bottlenecks that require special programming are matrix element evaluation, including both analytical two-electron integral formation, and numerical exchange correlation quadrature. As an illustration of the usefulness of the resulting algorithms for small-scale (single node or workstation) parallel calculations, Figure 5 shows the CPU timings and parallel speedups for a B3LYP/6-311G(3df,3pd) calculation on the glutamine molecule. Note that upon going from one core to two cores, the speedup is super linear: this reflects algorithmic improvements in the integral code that were made in the process of developing the parallel code.
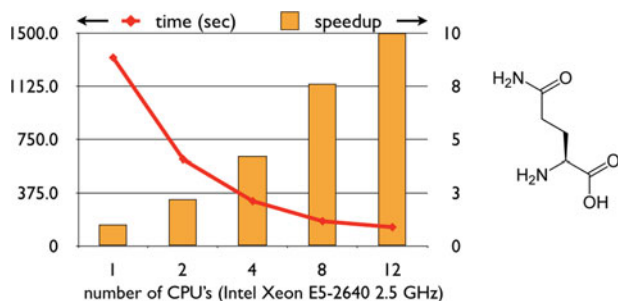
Figure 5. A plot of the computer timings and parallel speedups for calculations on the glutamine molecule (see 2-d structure at the right of the figure), for energy evaluation at the B3LYP/6-311(3df,3pd) level of theory.

OpenMP parallel capabilities have also been added for RI-MP2 calculations [153]. A novel algorithm that minimises disk transfers in the shared memory environment is employed, and all steps scaling higher than quadratic in system size are parallelised. Combining the OpenMP SCF and OpenMP parallel capabilities permits low elapsed job times for even quite large molecules in medium-sized basis sets. As an example of the usefulness of these algorithms for practical applications, Figure 6 shows two large molecular complexes from the L7 database [161]. The first, GCGC, is two guanine–cytosine base pairs that are arranged in a stacked Watson–Crick hydrogen-bonded arrangement as in DNA. The second, PHE, is a trimer of phenylalanine residues in a mixed hydrogen-bonded-stacked conformation. Figure 6 also shows the elapsed timings for the SCF and MP2 steps on a 64 core 2.3 GHz AMD Opteron 6300 series node, which indicate that the MP2 calculation is still less computationally demanding than the SCF step in these quite extended systems. These large 1000–1400 basis
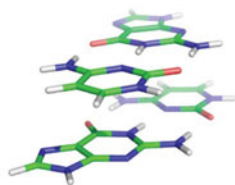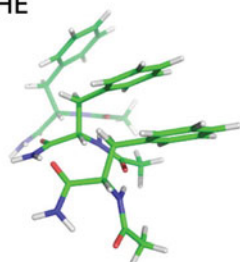
	basis functions	SCF time (hours)	RI-MP2 time (hours)
GCGC	1054	1.2	0.2
PHE	1413	2.8	0.6

Figure 6. Elapsed times for SCF and MP2 energy evaluation on two large complexes from the L7 database [161], using the aug-cc-pVDZ basis set, with integral thresholds of 10^{-14} and an SCF convergence criterion of 10^{-10}. The calculations were performed on a 64 core 2.3 GHz AMD Opteron 6300 series node.

function calculations with high precision (integral thresholds of 10^{-14} and SCF convergence of 10^{-10}) show elapsed times of only two to three hours. In addition, GPU code has been added for RI-MP2 energies [240,241] and gradients.

5. Walking on potential energy surfaces

In quantum chemistry codes, it has been common practice to provide sophisticated local optimisation methods [242] that permit optimisation to minima with emphasis on requiring as few gradient evaluations as possible, both by effective choice of coordinates, as well as guesses for Hessians, in addition to the optimisation procedure itself. Extensions of local optimisers, such as the partitioned rational function optimisation (P-RFO) method [243], are provided for converging to transition structures. Such methods, which are local optimisations to saddle points, walk downhill in all directions but the reaction coordinate, in which the walk is uphill. The P-RFO approach (and related methods) is very computationally efficient given an excellent initial guess, and an associated Hessian [244]. Recent developments provide additional sophisticated techniques that supplement these established tools, as discussed in the following subsections.

5.1. Growing and freezing string methods

If the initial guess for a transition structure is so poor that the associated Hessian has the incorrect character, then transition structure optimisations are quite likely to fail, and the cycle of guess structure, run search, fail, guess again, etc, can be labour intensive and frustrating. This difficulty can be substantially overcome if the reactant and product geometries, corresponding to initial and final minima, are known. In that case, automatic path-finding tools, such as the growing and freezing string methods, can characterise a reaction coordinate joining the end-points. The highest point on the pathway becomes an excellent initial guess for subsequent refinement of the transition structure.

The growing string method (GSM) is an iterative algorithm [245] for determining a set of intermediate structures that connect the reactant and the product via the intrinsic reaction coordinate (IRC). The GSM has been reimplemented recently [246], with the use of linear synchronous transit [247] to improve initial guessing. While formally very attractive, the GSM is still computationally quite expensive compared to the cost of a local optimisation to a transition structure. The freezing string method (FSM) [248] provides a much less expensive algorithm for determining a path with a specified number of intermediate structures (nodes) connecting reactant and product, starting like the GSM from both ends of the path, and adding nodes irreversibly until the two ends join. As a result of its non-iterative nature, the FSM cannot guarantee an IRC, but it is typically a quite reliable way to obtain a good initial guess for a transition

structure that can then be refined by conventional local search.

Neither the FSM nor GSM require Hessians. To further avoid the high cost of exact Hessian evaluation, additional new tools [249] have been added that provide two more important capabilities. First, algorithms that combine the known reaction coordinate and its curvature from the FSM (and refined by subsequent iterative diagonalisation using only gradients) enable the automatic construction of an initial Hessian for transition structure refinement at the end of an FSM calculation. Second, when a local optimisation has completed, the characterisation of the stationary point can also be performed by iterative diagonalisation using only gradients, to avoid Hessian evaluation at this step also. An example of the use of these tools is given at the end of this section.

5.2.   *Classical and quasi-classical trajectories*

Q-CHEM has contained *ab initio* classical trajectory methods for some years, based on an efficient Fock matrix extrapolation strategy [250]. For some purposes, however, purely classical dynamics are inadequate. As a simple example, consider simulating the infrared spectrum of a high-frequency mode such as an OH stretch in water clusters [251]: the vibrational amplitude would be much too small at room temperature by classical dynamics. Some (though not all!) of the limitations of classical trajectories may be overcome through the use of quasi-classical trajectories [252,253], which is now available in Q-CHEM [254]. An old but useful idea, quasi-classical trajectories are initialised with kinetic energy corresponding approximately to the appropriate quantum distributions based on normal mode analysis. The trajectories are run classically. Useful information can be obtained at short times (while at long times energy artificially flows from high-frequency modes to low-frequency ones), and a particularly useful case is the exploration of short trajectories that are launched from the highest energy intermediate transition structures in complex chemical reactions. As an example, quasi-classical trajectory studies of hydrocarbon cracking in zeolites have shown that a single high-energy transition structure can lead to multiple products (rather than a single path) [255].

5.3.   *Basin hopping for low-lying minima*
of clusters

In many chemical problems it is necessary to identify the global or low-lying minima on a complex potential energy surface. Characterisation of the structure of molecular clusters is one example that presents a challenge for standard structural optimisation techniques. The basin hopping method [256] is a combination of a Metropolis Monte Carlo sampling technique and a local search method, which has the effect of sampling energy basins instead of sampling
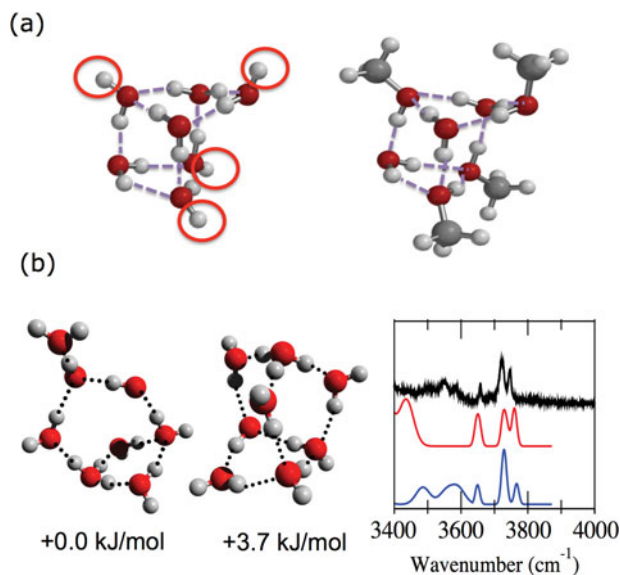

Figure 7.   (a) The global minimum energy structures of the $(H_2O)_7$ and $(H_2O)_3(CH_3OH)_4$ clusters. (b) The structures of the two lowest energy $(H_2O)_8^+$ clusters with the infrared spectra. The spectrum for the lowest energy isomer is shown in blue and the experimental spectrum is shown in black.

configuration space. In Q-CHEM, the basin hopping search also incorporates 'jumping', which allows the search to escape from a minimum by unconditionally accepting a series of moves.

Performing a basin hopping search in conjunction with quantum chemical methods removes the need to have a suitable empirical force field available and allows systems with more complex electronic structure or changes in electronic structure to be studied. Molecular clusters comprising water and methanol clusters have been studied at the B3LYP−D/6-31+G* level of theory [257]. The structures corresponding to the global minimum for the $(H_2O)_7$ and $(H_2O)_3(CH_3OH)_4$ clusters are illustrated in Figure 7, which shows the structures to be similar with the methyl groups of methanol occupying the sites of free hydrogens in the $(H_2O)_7$ cluster. Other studies have considered radical cation clusters including water [258,259] with a combination of DFT and MP2 methods. Low-energy structures that correspond to different characteristic structural motifs can be identified. Figure 7 also shows the two lowest energy isomers of the $(H_2O)_8^+$ cluster. Both of these isomers conform to a separated ion–radical pair structure, with H_3O^+ and OH that are not directly attached to each other. Also shown are the computed infrared spectra for the O–H stretching region. The spectrum for the lowest energy isomer is in excellent agreement with the spectrum measured by experiment [260], confirming that the correct isomer has been identified.
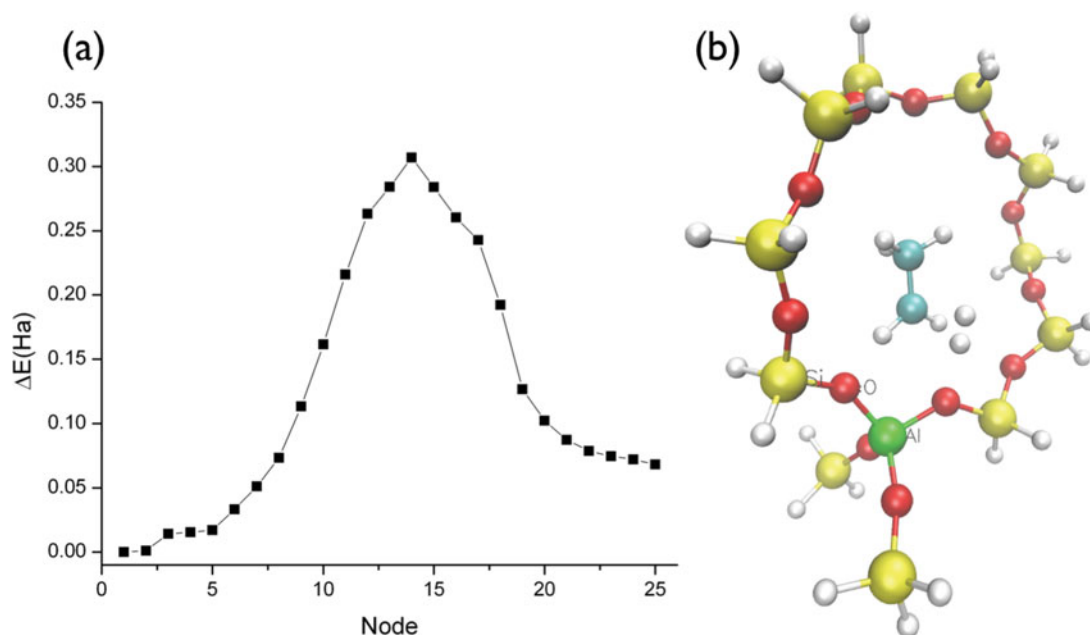
Figure 8. Illustration of a freezing string method (FSM) calculation on the transition structure for ethane dehydrogenation to ethene in the zeolite, H-MFI, modelled by a T12 cluster as described in the text. In panel (a), the relative energies of the calculated nodes of the FSM pathway are shown, beginning from the optimised structures of the reactant and the product. In panel (b), the final optimised transition structure is shown, which was calculated starting from the highest energy node on the FSM pathway.

5.4. Case study: ethane dehydrogenation transition structure in H-MFI zeolite

Cracking and dehydrogenation are competing reactions that alkanes undergo at Brønsted-acid sites within acidic zeolites. These monomolecular reactions can be used to probe the shape-selective behaviour in zeolite pores. There is a very large literature on electronic structure calculations on such systems, and prior to the development of economical methods for automatically locating transition structures, such as the FSM, the location of transition structures was labour intensive. In this example, the FSM TS search beginning with reactant and product geometries is used.

A cluster model consisting of 12 tetrahedral (T) atoms terminated with H is used, with the acid site located at the T12 position. The reactant state consists of ethane physisorbed at this acid site, and the product state consists of physisorbed ethene and H2. The T5 cluster consisting of the Al atom and four surrounding Si atoms is allowed to relax, and the remaining zeolite framework is fixed. The system is treated at the B3LYP/3-21G level of theory. The transition structure that is located is illustrated in Figure 8.

The first step in this method is the generation of a guess to the TS. The FSM is used with 20 nodes along the string, and 3 gradient relaxation steps per node. The maximum energy point along the FSM string is taken as the TS guess. The second step involves refining this guess to the correct TS using the partitioned-rational function optimisation

(P-RFO) method. For TS searches, P-RFO is more reliable if the Hessian at the TS guess is used as input. In order to avoid a full Hessian calculation, which can be expensive for large systems such as zeolite clusters, an approximate Hessian can be generated from the FSM output. The TS guess and the approximate reaction coordinate generated by the FSM can be used to iteratively calculate the lowest eigenvalue and corresponding eigenvector of the exact Hessian using a finite difference implementation of the Davidson method. This information can then be incorporated into a guess matrix as described elsewhere.

The first step, generation of the FSM reaction path, requires 83 gradients. An additional 10 gradients are required to generate the lowest eigenvalue and eigenvector of the Hessian to initiate the TS refinement, which itself required 167 gradients to converge to good tolerances. The first key point to be made is that the automatic generation of the TS guess via the FSM does not greatly affect the cost of the overall search (less than twice as expensive), yet has the great advantage of removing the need to generate the guess by hand (possibly multiple times, if first attempts are inadequate). A second point is that the automatic generation of a Hessian with the correct structure requires only 10 gradients vs. the equivalent of about 62 gradients done analytically. The third point is that the approximate Hessian performs comparably to the exact one in the TS search itself (it requires 186 gradients for the same convergence from the same guess using the exact Hessian).

6. Modelling extended environment

Classical modelling of an extended environment (a solvent, or a macromolecular framework for example) is an important aspect of modern quantum chemistry calculations. Q-CHEM provides a variety of low-cost methods, of varying complexity and sophistication, for incorporating a classical environment into a quantum-mechanical calculation of the molecule or region of primary interest. These methods include several dielectric continuum-based descriptions of a liquid solvent; mixed QM/MM calculations that can be performed using Q-CHEM as a stand-alone program or else via an interface [261] with the widely used 'CHARMM' MM program [262]; and the effective fragment potential (EFP) method [263], which can be used to parameterise a polarisable force field, in an automated way based on quantum chemistry calculations. In addition to these quantum/classical approaches, several fragment-based quantum chemistry models are also available [264], in which the entire (super)system is ultimately described quantum-mechanically, but in order to reduce the cost this is done one subsystem at a time, using a variety of methods to describe the coupling between different subsystems.

6.1. Continuum solvation

Dielectric continuum models of liquid solution have a long history in quantum chemistry calculations [265,266], where they are usually known as *polarisable continuum models* (PCMs). PCMs model bulk electrostatics by treating the solvent as a homogeneous dielectric continuum characterised by a single parameter, ε: the dielectric constant. Q-CHEM includes several of the most recent innovations in this area, including a sophisticated treatment of continuum electrostatics that is known variously as the *integral equation formalism* (IEF-PCM) [267] or the *surface and simulation of volume polarisation for electrostatics* [SS(V)PE] model [268]. (The two are formally equivalent at the level of integral equations [269,270], but there are subtle yet important implementation differences, as discussed in [271].)

For high-dielectric solvents such as water, the much simpler conductor-like model (C-PCM) [272,273] affords nearly identical solvation free energies as compared to IEF-PCM/SS(V)PE, differing formally only by terms of $\mathcal{O}(\varepsilon^{-1})$ that are negligible for $\varepsilon \gtrsim 50$ [271]. Mathematically, C-PCM has the form [273]

$$\mathbf{Sq} = -f(\varepsilon)\,\mathbf{v} \tag{1}$$

where $\mathbf{Sq}$ (the electrostatic potential of the induced surface charge) is proportional to $\mathbf{v}$, the solute's electrostatic potential at the solute/continuum interface. The proportionality factor,

$$f(\varepsilon) = \frac{\varepsilon - 1}{\varepsilon + x}\,, \tag{2}$$

has been a source of much discussion in the literature [273–276], specifically with respect to whether the optimal choice is $x = 0$ [274] (consistent with the Born model) with $x = 1/2$ [277] (a compromise between Born's model of a charge in a sphere and Onsager's model of a dipole in a sphere). The choice is obviously inconsequential in high-dielectric ($\varepsilon \gg 1$) solvents, but in non-polar solvents the choice $x = 1/2$ proves to be somewhat more accurate as compared to experiment, at least when non-electrostatic terms are included as well [273]. Equation (1), with $x = 1/2$, was originally suggested by Klamt and Schüürmann [277], who called it the *conductor-like screening model* (COSMO). Nowadays, however, 'COSMO' implies a model based on Equation (1) but with an explicit correction for outlying charge [275,276]. (On the other hand, even C-PCM includes an *implicit* correction for outlying charge, as shown by Chipman [269].)

A C-PCM description of the solvent is available for excited-state TDDFT calculations as well [130], including its analytic gradient and Hessian. Together, these methods facilitate efficient solution-phase geometry optimisations and harmonic frequency calculations for molecules in excited electronic states.

One crucial aspect of the implementation of any PCM is the construction of a molecule-shaped 'cavity' that defines the interface between the atomistic solute and the continuum solvent. A formally appealing way to construct the cavity is to let it coincide with an isocontour of the quantum-mechanical solute electron density [278], and such a construction is available in Q-CHEM for use with SS(V)PE [279]. Unfortunately, the analytic energy gradient for such a construction has yet to be developed, and at present, carefully parameterised, bond-connectivity-dependent atomic radii can surpass the accuracy of an isodensity cavity when it comes to computing solvation free energies [280]. (Recent attempts to incorporate non-electrostatic terms into the isodensity construction show great promise for high accuracy with minimal parameterisation [281,282], but these corrections are not yet available in Q-CHEM.)

For these reasons, the vast majority of PCM calculations use a cavity construction that is based in some way on atom-centred van der Waals spheres. Because these spheres must be discretised onto a grid for practical calculations, such an approach suffers from discontinuities in the energy and forces as the atoms are allowed to move, e.g., in a geometry optimisation [284]. This ubiquitous problem is avoided by Q-CHEM's intrinsically smooth implementation of both IEF-PCM and C-PCM [271,284,285]. This implementation passes the stringent test of conserving energy in *ab initio* molecular dynamics simulations of solution-phase molecules, even for difficult cases such as intramolecular proton transfer in aqueous glycine, where the shape of the cavity changes drastically as the proton is shuffled between carboxylate and amino moieties [285].

Table 6. Mean unsigned errors (MUEs, in kcal/mol) for solvation free energies in water and in 17 organic solvents, from [283].

Solute class	No. data points	SM8 MUE (kcal/mol)
All neutrals	940	0.6
All ions	332	4.3
All cations	124	3.9
All anions	208	4.6
Aq. neutrals	274	0.6
Nonaq. neutrals	666	0.6
Aq. ions	112	3.2
Nonaq. ions	220	4.9

Table 7. Mean unsigned errors (MUEs, in kcal/mol) for solvation free energies, for models that include non-electrostatic interactions. (Adapted from [288]; copyright 2009 American Chemical Society.)

Solute class	No. data points	MUE (kcal/mol)		
		IEF-PCM+ non-elst.[a]	COSMO-RS[b]	SM8
All neutral[c]	2346		0.5	0.6
17 organic solvents	960		0.6	0.6
3 organic solvents[d]	960	0.6		0.6
Aq. solvation	284	1.0	0.6	0.6

[a]Includes non-electrostatic terms [286,287].
[b]Requires the COSMOTHERM software in addition to Q-CHEM.
[c]Includes all 91 solvents and 2346 data points used to parameterise SM8.
[d]Octanol, CHCl$_3$, and CCl$_4$.

The aforementioned PCMs, however, treat only the bulk electrostatic contributions to solvation, neglecting other contributions such as dispersion, exchange repulsion, and solute-induced changes in the solvent structure. Although non-electrostatic corrections to PCMs can be put in 'by hand' [286,287] to obtain accurate free energies of solvation [288], a more universal approach is offered by the so-called SMx models developed by Cramer and Truhlar [283]. The SMx models use a variety of macroscopic solvent descriptors (surface tension, refractive index, acid/base parameters, etc.) to parameterise non-bulk electrostatic corrections to a generalised Born treatment of bulk electrostatics [289,290], and are designed to work in a black-box way for any solvent. Q-CHEM includes two of the more recent versions of the SMx approach: SM8 [291] and SM12 [292]. Both models afford similar statistical errors in solvation free energies [292], but SM12 does lift an important restriction on the level of electronic structure that can be combined with these models. Specifically, the generalised Born model for electrostatics that is employed in SM8 is based upon a variant of Mulliken-style atomic charges, and is therefore parameterised only for a few small basis sets, e.g., 6-31G*, whereas SM12 uses charges that are stable with respect to basis-set expansion (namely CM5 charges [293]) and is therefore available at any level of electronic structure theory.

Mean statistical errors in solvation free energies (ΔG_{298}) vs. experiment are shown in Tables 6 and 7 for several implicit solvent models. Results in Table 6 demonstrate that the SM8 model achieves sub-kcal/mol accuracy for neutral molecules, although average errors for ions are more like ~4 kcal/mol [283]. Non-electrostatic terms appropriate for IEF-PCM are available for a few solvents [286,287], and when these are included, the 'IEF-PCM+non-elst.' errors (Table 7) are comparable to those obtained using SM8 [288]. Also shown in Table 7 are results from the COSMO-RS model (where RS stands for 'real solvent') [294,295]. This model yields error statistics that are essentially identical to those exhibited by SM8, but requires external software in addition to Q-CHEM.

6.2. QM/MM and fragment methods

For serious QM/MM applications, significant developments have also occurred with respect to Q-CHEM's ability to interface with external classical simulation packages, particularly the CHARMM program. First, major strides were made in the area of QM/MM normal mode analysis. In 2009, full QM/MM analytic second derivatives were implemented in Q-CHEM (stand-alone and coupled to CHARMM) [296]; both restricted and unrestricted HF and DFT methods are supported. This was closely followed by the parallelisation of these full QM/MM Hessian calculations and extension to the mobile block Hessian formalism, significantly reducing CPU and memory requirements for these intensive calculations [297]. Complementing Q-CHEM/CHARMM support for QM/MM dielectric approaches (see also QM/MM/PCM below), the solvent macromolecule boundary potential method has also been interfaced to Q-CHEM [298,299]. Last, but not least, a user-friendly Web interface that facilitates the graphical set-up of QM/MM calculations (i.e., Q-CHEM/CHARMM) was also developed [300]. It is anticipated that this will receive significant enhancements in the near future and tie closely into IQMOL, which is discussed in Section 9.

In addition, major progress has been made since v. 3.0 towards making Q-CHEM a versatile, stand-alone QM/MM program [38,301], without the need to interface with CHARMM or any other classical MD package. Notable features of the stand-alone QM/MM package include the availability of several widely used force fields (AMBER, CHARMM, OPLS) with an option to add user-definable force field parameters. QM/MM functionality is available for all QM models implemented in Q-CHEM, including excited-state methods insofar as correlated post-HF wave function models or time-dependent DFT can be based on a reference determinant that has been polarised by the MM environment. For ground-state calculations, periodic boundary conditions are available based on a novel implementation of Ewald summation for QM/MM calculations

[301]. Alternatively, the PCM solvation models discussed in Section 6.1 can be used as boundary conditions for a QM/MM calculation. In this case, the solute/continuum interface is defined by the (potentially sizable) MM region of the calculation, such that the cubic-scaling PCM equations potentially become the bottleneck of the calculation, exceeding the QM cost! To facilitate large-scale QM/MM/PCM calculations, Q-CHEM therefore includes a linear-scaling, scalable-parallel conjugate gradient solver for the PCM equations [305]. Significant progress towards enhancing the stand-alone QM/MM functionality is anticipated in the near future.

Q-CHEM also provides a more sophisticated way to account for environment effects on the electronic structure of a solute, by using the EFP method. The EFP method is a first-principles-based model that was originally designed to describe aqueous environments [306,307]. It was later extended to general solvents and biological environments [263,308,309]. The interaction energy between EFP fragments is modelled as a sum of Coulomb, polarisation, dispersion, and exchange-repulsion terms, all of which are derived as truncated expansions in terms of intermolecular distance and overlap integrals. The accuracy of the EFP method was tested on the S22 and S66 data-sets for non-covalent interactions [302]. The results shown in Table 8 demonstrate that EFP is similar in accuracy to MP2 and the M06 density functional and is superior to classical force fields and most density functionals not corrected for dispersion interactions.

EFP is interfaced with the SCF, CIS/TDDFT, and CC-MAN/CCMAN2 modules, allowing ground and excited state calculations in the presence of polarisable environments [310–312]. Electrostatic and polarisation EFP terms in QM/EFP calculations modify the electronic Hamiltonian of the quantum region to affect the shapes and energies of the molecular orbitals (MOs) of a solute. Each excited state interacts differently with the polarisable environment. This effect is accounted for by computing additive energy corrections to the excitation energies [310]. The combination of first-prinicple polarisable explicit solvents with the EOM-CC family of methods is a unique feature of Q-CHEM, enabling state-of-the art calculations of solvatochromic effects and redox processes [312,313]. To sum up, the major differences between the QM/EFP and QM/MM schemes are: (1) more accurate and detailed description of the electrostatic interactions in EFP using distributed multipoles up to octopoles versus the partial charge representation used in typical MM; (2) polarisable environment in EFP induces self-consistent response to the electronic wave function of the quantum region, while most classical force fields are not polarisable.

EFP is a fragment-based rather than atom-based potential. Each effective fragment contains a set of pre-defined parameters. Parameters for any fragment may be generated in the GAMESS package [314] in a special type of

Table 8. Mean unsigned errors (in kcal/mol) of the total interaction energies for hydrogen bonded (HB), dispersion dominated (DISP), mixed (MIXED) complexes and the whole group (ALL) of the S22 data-set by EFP, molecular mechanics force fields, HF, DFT, and *ab initio* methods. From [302] and references therein, except for the XSAPT values [303,304].

Method	HB	DISP	MIXED	ALL
EFP	1.97	0.48	0.34	0.91
Force fields				
Amber	4.79	0.98	0.98	2.16
OPLSAA	4.59	1.04	0.57	2.02
MMFF94	3.75	0.88	0.59	1.70
HF and DFT				
HF	3.29	7.24	3.15	4.56
B3LYP	1.77	6.22	2.64	3.54
PBE	1.13	4.53	1.66	2.44
M05	1.26	3.16	1.09	1.84
M06	0.89	0.99	0.67	0.85
M06-2X	0.73	0.36	0.32	0.47
BLYP-D3				0.23
ωB97X-D				0.22
Correlated methods				
MP2	0.24	1.69	0.61	0.88
SCS-MP2	1.54	0.55	0.37	0.80
SCS-CCSD	0.40	0.23	0.08	0.24
XSAPT-based methods				
XSAPT(KS)+D1	0.73	0.38	0.52	0.53
XSAPT(KS)+D2	0.72	1.18	0.52	0.82
XSAPT(KS)+D3	0.76	0.67	0.38	0.61
sd-XSAPT	0.33	0.30	0.32	0.32

run (MAKEFP run). The Q-CHEM distribution contains a library of fragments with prepared and tested potentials (typical solvents, DNA bases, molecules from S22 and S66 data-sets). Effective fragments are kept rigid in all computations. The QM/EFP formalism can be extended to biological systems. For that, a biological polymer is split into and represented by a set of individual effective fragments. Scripts automating preparation of the fragments and parameters are provided within the Q-CHEM distribution. The Q-CHEM implementation of the EFP method is based on the stand-alone EFP library *libefp* [315] and will benefit from all future updates and improvements to the EFP algorithms.

Other fragment-based methods for non-covalent interactions that are available in Q-CHEM include an electrostatically embedded many-body expansion [316]. This method is based on a truncation of the traditional many-body expansion,

$$E = \sum_I^N E_I + \sum_I^N \sum_{J>I}^N \Delta E_{IJ}$$
$$+ \sum_I^N \sum_{J>I}^N \sum_{K>J}^N \Delta E_{IJK} + \cdots , \qquad (3)$$

in which E_I represents the energy of monomer I, $\Delta E_{IJ} = E_{IJ} - E_I - E_J$ is a two-body correction for dimer IJ, etc. The idea is to truncate Equation (3) at some number of 'bodies' $n \ll N$, and to accelerate convergence (with respect to n) by performing the monomer (E_I), dimer (E_{IJ}), trimer (E_{IJK}), ... calculations in a point-charge representation of the remaining monomer units. These point charges can be obtained, e.g., as Mulliken charges or as charges fitted to the monomer electrostatic potentials (ChElPG charges [317]). Due to the highly non-linear scaling of quantum chemistry methods, the cost of performing, e.g., $N(N - 1)(N - 2)/6$ distinct trimer calculations, $N(N - 1)/2$ distinct dimer calculations, and N distinct monomer calculations may be far less than the cost of performing an electronic structure calculation on the entire non-covalent supersystem. The subsystem calculations can be performed at any level of theory, and electrostatically embedded two- and three-body expansions are often reasonably faithful to supersystem results computed at the same level of theory [264,316,318].

A fragment-based method for non-covalent interactions that is currently unique to Q-CHEM is an extended (cluster) version of symmetry-adapted perturbation theory [264,303,304,319,320]. This so-called XSAPT method generalises the traditional SAPT methodology [321] to clusters of arbitrary size, treating many-body polarisation effects in a self-consistent way but approximating other non-covalent interactions (exchange and dispersion) in a pairwise-additive but *ab initio* fashion. XSAPT extends SAPT-style energy decomposition analysis to clusters containing more than two monomer units [304]. For a cluster consisting of N monomer units, the cost of an XSAPT calculation is about the same as $N(N - 1)/2$ second-order dimer SAPT calculations, each of which is MP2-like in cost. Second-order SAPT works well for non-covalent clusters whose interactions are dominated by polarisation (induction) and electrostatics, but inherits MP2's problems with overestimating dispersion energies in the basis-set limit. For dispersion-bound systems, good results are only obtained by carefully choosing a small basis set to exploit error cancellation [319,320].

This unhappy state of affairs is remedied by replacing the MP2-like dispersion and exchange-dispersion terms in SAPT with empirical atom–atom dispersion potentials, which also has the effect of reducing the cost from fifth-order to third-order scaling [303,304]! The resulting method is called XSAPT(KS)+D, where the 'KS' refers to the fact that KS-DFT is used for the monomers. The cost therefore scales like DFT with respect to the size of the monomer units [303], while scaling only quadratically with respect to the number of monomer units, making it cheaper than supersystem DFT already for as few as $N = 2$ monomers [303]. At the same time, the method exhibits sub-kcal/mol accuracy (relative to complete-basis CCSD(T) benchmarks) for non-covalent interactions [303,304], as shown in Table 9 for three successively improved versions

of the empirical dispersion potential (D1, D2, and D3). Also shown are very recent results in which second-order dispersion is retained but empirically scaled, as suggested in [323]. Mean unsigned errors (MUEs) for various subsets of the S22 data-set are shown in Table 8, from which it is clear that these methods provide outstanding performance for both systems that are dominated by electrostatics and induction (the HB subset) as well as those whose binding is dominated by dispersion.

7. Energy and electron transfer

7.1. Energy transfer: direct Coulomb and exchange couplings

Excitation energy transfer (EET) is a process where one electronically excited molecule or fragment passes its excitation energy to another. In the singlet states, it is the widely used Förster energy transfer [324]. EET in triplet states is seen in triplet quenching processes [325], as well as artificial light-emitting systems utilising phosphorescence [326,327]. Fermi's golden rule has the rates of these processes proportional to the square of an electronic coupling factor, which is the off-diagonal Hamiltonian matrix element for the diabatic states (i.e., locally excited states [328]).

Computational schemes that offer total EET couplings such as the fragment excitation difference and the fragment spin difference has been available in Q-CHEM for several years [329–331]. In this revision, we have included the option to compute the Coulomb and exchange couplings to further dissect the total coupling and derive physical insights into its origin [332]. In the derivation of the coupling for singlet EET (SEET), [324,333–335] a first-order perturbation expansion is often used. It can be shown that the electronic coupling for singlet EET contains three contributions,

$$V^{\text{SEET}} = V^{\text{Coul}} + V^{\text{exch}} + V^{\text{ovlp}}, \tag{4}$$

while the corresponding breakdown for triplet EET (TEET) is [331]:

$$V^{\text{TEET}} = V^{\text{exch}} + V^{\text{ovlp}}. \tag{5}$$

In Equation (4), V^{Coul} is the Coulomb coupling that arises from the Coulomb interaction between electronic transitions,

$$V^{\text{Coul}} = \iint d\mathbf{r}_1 d\mathbf{r}_2 \, \frac{\rho_D^{\text{tr*}}(\mathbf{r}_1) \rho_A^{\text{tr}}(\mathbf{r}_2)}{|\mathbf{r}_1 - \mathbf{r}_2|}. \tag{6}$$

V^{exch} in both Equations (4) and (5) is the exchange coupling,

$$V^{\text{exch}} = - \iint d\mathbf{r}_1 d\mathbf{r}_2 \, \frac{\gamma_D^{\text{tr*}}(\mathbf{r}_1, \mathbf{r}_2) \gamma_A^{\text{tr}}(\mathbf{r}_1, \mathbf{r}_2)}{|\mathbf{r}_1 - \mathbf{r}_2|}, \tag{7}$$

Table 9. Mean unsigned errors (MUEs) and maximum errors, both in kcal/mol, with respect to CCSD(T)/CBS benchmarks for the S22 [82,83], S66 [84,85], and CHB15 data-sets [322], using three generations of XSAPT(KS)+D as well as XSAPT(KS) with scaled second-order dispersion, sd-XSAPT(KS). The Kohn–Sham functional used is LRC-ωPBE [37], with ω tuned in a monomer-specific way to achieve the condition that ε_{HOMO} equals minus the ionisation potential [304].

Method	Basis set	S22		S66		CHB15	
		MUE	Max	MUE	Max	MUE	Max
XSAPT(KS)+D1	ha-DZ[a]	0.53	(1.16)	0.29	(1.07)	0.98	(1.96)
XSAPT(KS)+D2	ha-TZVPP[b]	0.82	(4.23)	0.39	(3.32)	1.43	(4.30)
XSAPT(KS)+D3	hp-TZVPP[c]	0.61	(1.91)	0.45	(1.96)	0.89	(2.39)
sd-XSAPT(KS)	6-31G(d,2p)	0.32	(0.72)	0.37	(0.97)	0.77	(2.21)

[a]cc-pVDZ for hydrogen and aug-cc-pVDZ for other atoms.
[b]def2-TZVPP, with diffuse functions from aug-cc-pVTZ for non-hydrogen atoms.
[c]def2-TZVPP, with diffuse functions from 6-311+G for non-hydrogen atoms.

which is the Dexter exchange coupling that arises from the indistinguishability of the electrons in many-electron wave functions [333]. $\gamma^{tr}(\mathbf{r}, \mathbf{r}')$ in Equation (7) is a one-particle transition density matrix. $\rho^{tr}(\mathbf{r})$ in Equation (6) contains diagonal elements of the transition density matrix: $\rho^{tr}(\mathbf{r}) \equiv \gamma^{tr}(\mathbf{r}, \mathbf{r})$. The remaining contributions to EET couplings, such as the term V^{ovlp} arising from the overlap of donor–acceptor orbitals, and the influence of ionic-CIs have also been discussed in the literature [332,336,337].

In the condensed phase, the polarisability of surrounding molecules affects the Coulomb part of the EET coupling of the chromophores. A quantum mechanical model was formulated through a general TDDFT framework [335] for the polarisability effect in SEET coupling. The solvent effect on the Coulomb coupling was treated with a continuum solvent model [338]. Such solvent effects have been studied for photosynthetic light-harvesting systems [339,340].

Q-CHEM's direct coupling scheme for electron transfer coupling is now extended for the Coulomb and exchange couplings in EET (V^{could} and V^{exch} Equations (6) and (7)). The donor and acceptor transition densities are calculated separately from CIS or TDDFT calculations, and the Coulomb and exchange couplings are calculated using the efficient two-electron integrals in Q-CHEM. The solvent polarisation effect on the Coulomb coupling is also implemented in this revision, using the efficient PCM kernel in Q-CHEM (Section 6.1). Such results allow one to analyse the physical contributions to the EET coupling [329,331,332].

7.2. Constrained DFT

One way to treat electronic energy transfer and electron transfer processes is to construct appropriate diabatic states [341]. In the context of DFT, one appealing way to do this is through *constrained* DFT (CDFT) [342]. One minimises the energy of the system subject to chemically or physically motivated constraints on the density [343,344]. For example, in electron transfer, one might constrain the net charge on a fragment of the molecule [345,346], or for magnetic systems one might constrain the net spin [347]. These states then provide a basis for describing reactant- and product-like states for electronic reactions. From the computational point of view, because CDFT is variational, the energies and analytic forces are easily computed at a cost that is not much higher than standard DFT. Q-CHEM has the ability to apply multiple simultaneous constraints to the system for any density functional. The result is that, in addition to specifying the atomic coordinates, one also has the ability to specify the net charges and/or spins on multiple fragments within a molecule or supramolecular assembly.

In addition to energies of these diabatic-like states, one also would like to be able to compute the electronic coupling between two CDFT states. This can be done using a simple approximation involving the KS orbitals [348]. The resulting electronic coupling can then be computed in a fraction of the time of the CDFT calculations themselves. The CDFT idea can also be applied in many contexts beyond electron transfer. Notably, the CDFT solutions bear a strong resemblance to valence bond configurations, which leads to the realisation that CDFT states can be a good way of using DFT for problems that are inherently multi-reference [349,350]. The basic idea is to converge several CDFT states (that play the role of the active space in an MCSCF or CASSCF calculation) and then build the Hamiltonian as a matrix, using the energies of the states and the couplings between them. One then does a small CI calculation to account for the influence of these different valence bond-like states on the total wave function. This CDFT-CI method is able to describe conical intersections between the excited state and the ground state [351] and recently analytic gradients of this method have also been implemented [352].

7.3. Localised diabatisation

As an alternative to direct coupling or constrained DFT, meaningful diabatic states can also be computed via

localised diabatisation. In particular, Q-CHEM now allows the user to transform CIS or TDDFT/TDA adiabatic excited states according to either Boys [353] or Edmiston–Ruedenberg [354] localised diabatisation. Diabatic states $\{|\Xi_I >\rangle\}$ can be generated from multiple ($N_{\text{states}} \geq 2$) adiabatic states

$$|\Xi_I\rangle = \sum_{J=1}^{N_{\text{states}}} |\Phi_J\rangle\, U_{ji} \qquad I = 1 \ldots N_{\text{states}}, \qquad (8)$$

and the user must decide only which adiabatic states $\{|\Phi_I >\rangle\}$ should be transformed. In analogy to orbital localisation, Boys localised diabatisation prescribes maximising the charge separation between diabatic state centers, whereas ER localised diabatisation prescribes maximising the total self-interaction energy. Note, however, that both methods are completely invariant to choice of orbitals. These methods can be justified by assuming a slow solvent coordinate that is moderately coupled to an electronic subsystem. Boys localisation then assumes that the solvent coordinate yields an electric field that is linear in space (and, in effect, is a multi-state generalisation of generalised Mulliken–Hush [353]), while ER localisation assumes that that solvent takes the form of an isotropic linear dielectric medium. While Boys localisation can be applied safely for ET, ER localisation can be applied safely for both ET and EET. Q-CHEM also allows a third option, BoysOV [355], specifically for EET; according to BoysOV, one performs Boys localised diabatisation separately for the virtual (particle) and occupied (hole) components of the dipole operator.

Finally, for energy transfer, it can be helpful to understand the origin of the diabatic couplings. Thus, for adiabatic CIS excited states, Q-CHEM now provides the functionality to decompose the diabatic coupling between diabatic states into Coulomb (J), exchange (K), and one-electron (O) components [356]:

$$|\Xi_I\rangle \equiv \sum_{ia} t_i^{Ia}\, |\Phi_i^a\rangle$$

$$\langle \Xi_P | H | \Xi_Q \rangle = \underbrace{\sum_{iab} t_i^{Pa} t_i^{Qb} F_{ab} - \sum_{ija} t_i^{Pa} t_j^{Qa} F_{ij}}_{O} \\ + \underbrace{\sum_{ijab} t_i^{Pa} t_j^{Qb} (ia|jb)}_{J} + \underbrace{- \sum_{ijab} t_i^{Pa} t_j^{Qb} (ij|ab)}_{K}$$

7.4. Derivative couplings

As one last tool for studying electronic relaxation and non-adiabatic dynamics, Q-CHEM now provides the functionality to compute derivative couplings between CIS excited states, $d_{IJ}^{\alpha} \equiv \langle \Phi_I | \frac{\partial}{\partial R^{\alpha}} | \Phi_J \rangle$. Within the context of an adiabatic representation, derivative couplings are the leading terms that break the Born–Oppenheimer approximation [357]; indeed, they are infinite at a conical intersection. As detailed in [358], these couplings can be computed with or without electron translation factors; without electron translation factors, the derivative couplings are not translationally invariant. Q-CHEM provides derivative couplings for the user with and without such factors.

7.5. Transport and molecular electronics

Molecular scale electronics, where either one or a few molecules bridge two conducting electrodes, is a focus of considerable research activity. These large-scale efforts have led to impressive advances in the fabrication of molecular bridges, measurement of current–voltage relations, and associated computational modelling [359–367]. Much of the interest stems from the prospect of fabricating electronic devices that are tunable at the molecular level.

In molecular bridges the electronic density is affected by the coupling to biased electrodes. Accordingly, the electrodes' electronic band structure is projected onto the otherwise discrete electronic levels of the molecules. Most computational approaches to model electron transport are based on viewing the conductivity as due to scattering events through the molecule, where electrons are transmitted to the bridge broadened electronic states [368–372]. This picture of current follows the seminal work of Landauer, where the quantum transport function is integrated over the energies around the Fermi level as set by the voltage bias [373–375]. In state-of-the-art treatments, the electronic density of an electrode-coupled system is evaluated by the single particle Green's function (GF) formalism with DFT for describing the electronic interactions within the bridge. The GF formalism is then used to calculate the transmission function [376,377]. The same approach can be extended to treat biasing conditions by a self-consistent procedure for calculating the electronic density coupled to the biased electrodes using non-equilibrium GF formalism [371,378,379].

The quantum transport utility in Q-CHEM (called T-CHEM) can calculate the transmission function at any implemented variational level. T-CHEM implements the Green's function expressions used for calculating the transmission function [380–392]. An important modelling aspect is to set the self-energies (SEs) that represent the coupling to the extended system posed by the electrodes. Here, the extent of the electronic screening has to be decided. Namely, the molecular bridge region is usually defined to include several repeating units of the electrode beyond the surface layer [393,394]. In T-CHEM, the SE can be based on precalculated electrode models or on subregions within the supermolecule that are provided in the $ *molecule* section which are calculated on the fly. While the flexibility in setting the SE models is a great advantage, it has to be used with great care to avoid artefacts [393,394].
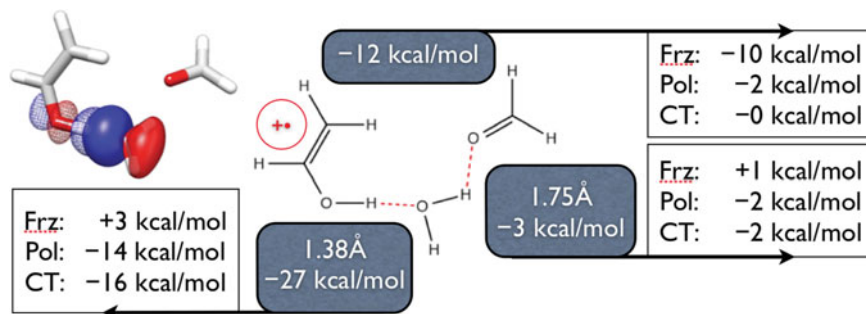
Figure 9. EDA results (from large basis DFT calculations) for the ternary complex of the vinyl alcohol cation, formaldehyde, and water that results from photoionising glycerol, HOCH$_2$-CHOH-CH$_2$OH. Its stability arises from two strong interactions. The largest is a 27 kcal/mol H-bond between water and the vinyl alcohol cation. This type of H-bridged ion–molecule interaction is often assumed to be electrostatic, but the EDA shows it is at least 50% CT in origin. The O lone pair donor orbital (bold), and HO σ^* acceptor orbital (faint) pair are shown at the top left. The second strong interaction is a longer-range electrostatic (charge-dipole, frozen-dominated) interaction between the vinyl alcohol cation and formaldehyde with little CT (see top right).

8. Analysis

8.1. *Energy decomposition analysis*

Understanding the origin of intermolecular or intramolecular interactions in terms of physically interpretable components is the goal of energy decomposition analysis (EDA) methods. Such components typically include permanent electrostatics, corresponding to interactions between charges and/or multipole moments, induced electrostatics associated with polarisation, Pauli repulsions associated with interactions between filled orbitals, and dative or donor acceptor interactions associated with interactions between filled and empty orbitals. By far the best-known EDA approach is the natural bond orbital (NBO) suite of methods due to Weinhold and co-workers [395–398], which Q-CHEM supports via a standard interface to the current version of the NBO package.

In addition, Q-CHEM contains the absolutely localised molecular orbital (ALMO) EDA [399], as a built-in method. The ALMO EDA is a descendent of the Kitaura–Morokuma EDA [400] (which is perhaps the first EDA method), and uses the same definition of the frozen interactions. It is also closely related to the block-localised wave function EDA [401,402] because both approaches use the same variational definition of the polarisation energy that is an upper limit to the true extent of polarisation [403]. A distinctive advantage of the ALMO-EDA is that the charge-transfer contribution is separated into pairwise additive contributions associated with forward and back-donation, and a non-pairwise decomposable higher order contribution, which is very small for typical intermolecular interactions. The ALMO-EDA is implemented for open-shell [404] as well as closed-shell fragments [399], and uses the efficient ALMO-SCF method [405] as its underlying computational engine.

In addition to the energy decomposition, the ALMO-EDA provides a means to automatically generate the pairs of orbitals (donor and acceptor) that are responsible for da-

tive interactions, which can be visualised and chemically interpreted [406]. As an example of the application of the ALMO-EDA, Figure 9 shows the principal intermolecular interactions associated with the trimeric complex between the vinyl alcohol cation, water, and formaldehyde. This triplex was recently identified by computational and experimental evidence [407] as being the principal intermediate that results from photoionisation of the glycerol molecule, before fragmentation occurs. The remarkable stability of the complex is due to two very strong intermolecular interactions. The first one has the character of a very short, strong hydrogen bond, involving charge transfer from a water lone pair towards the vinyl alcohol cation, in addition to strong polarisation effects. The second one is primarily an electrostatic interaction, involving both permanent and induced components, between the vinyl alcohol cation and formaldehyde. The strength of the ALMO-EDA is in clearly distinguishing the different character of the two strongest interactions.

8.2. *Natural transition orbitals*

The canonical MOs are seldom a good basis for conceptual understanding of electronic transitions, especially for HF (as opposed to KS) MOs, where the virtual orbitals formally describe electron-attached states rather than bound excitations, leading to significant mixing of the canonical MOs in the excited-state wave function. Density differences or attachment/detachment densities [408], both long available in Q-CHEM, are often more helpful, but densities lack the nodal structure that sometimes provides important information about the character of an excited state. An important class of examples are the Frenkel exciton states in a system composed of multiple, electronically coupled chromophore units. These excitons are delocalised over more than one chromophore unit, leading to attachment and detachment
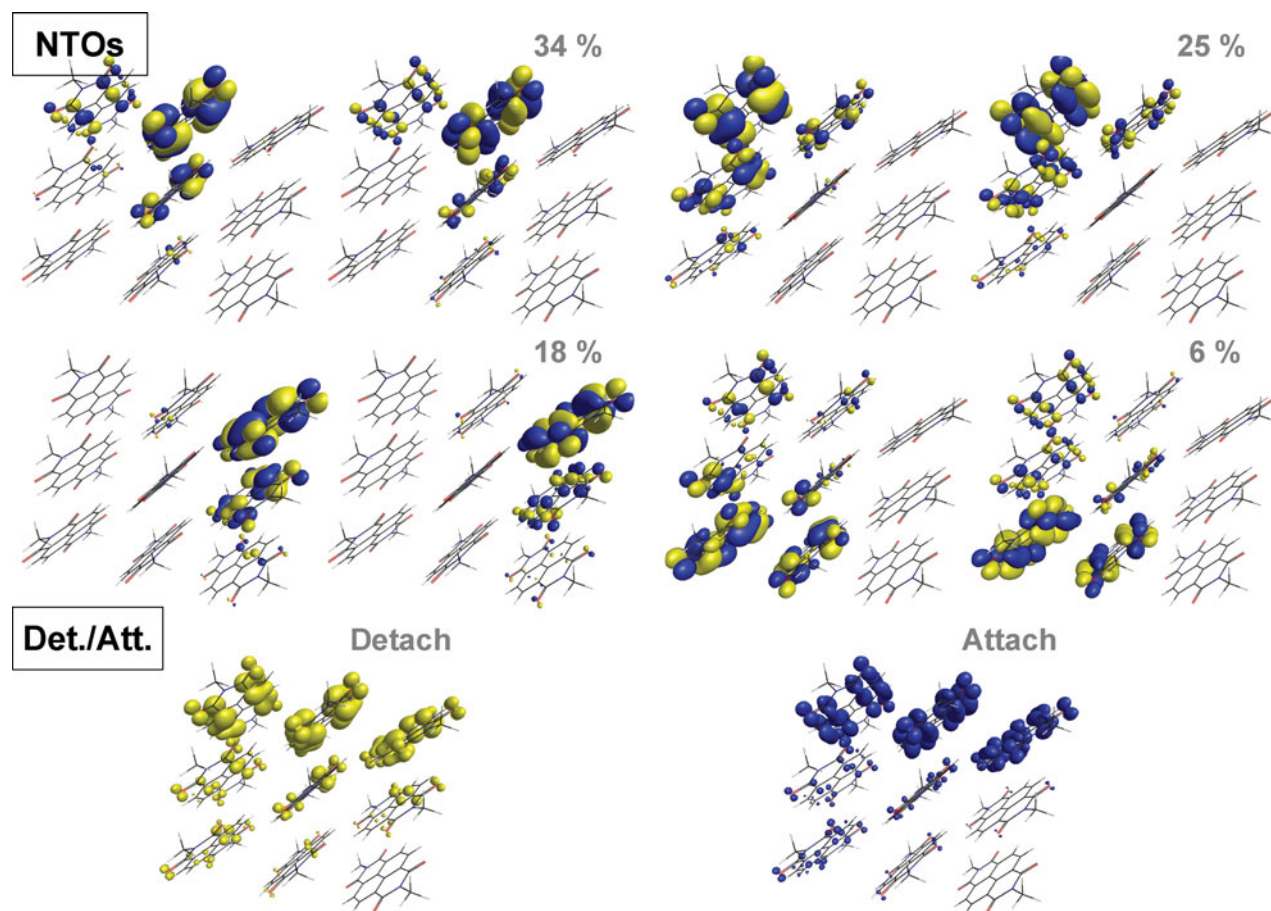
Figure 10. NTOs with largest amplitude, and attachment/detachment densities, for a Frenkel exciton state in a nine-unit model of the self-assembling nanotube described in [412]. The chromophore unit is a derivative of naphthalenetetracarboxylic acid diimide.

densities that are both highly delocalised, and each of which occupies approximately the same region of space. Nodal information is extremely useful in interpreting the character of such an excited state, which is often (at a qualitative level) simply a linear combination of optically allowed transitions on the monomer units [38].

Analysis of these and other excited states is greatly simplified by constructing *natural transition orbitals* (NTOs) [409–411]. For a given excited state, these orbitals amount to the unitary transformations of the occupied and virtual MOs that provide the best possible particle/hole picture of that state, in the sense of having a dominant occupied/virtual transition. The attachment/detachment densities are recovered as the sum of the squares of the particle/hole NTOs, but the NTOs are orbitals (not densities) and thus contain phase information. This is helpful in assigning diabatic character ($\pi\pi^*$, $n\pi^*$, etc.) to excited states in complex systems. An example is shown in Figure 10, which depicts both NTOs and attachment/detachment densities for a particular exciton-type state of a nine-chromophore model of a self-assembling organic nanotube [412]. Both the attachment and detachment densities are delocalised over essentially

the same four chromophores. Inspection of the four occupied/virtual NTO pairs with largest amplitudes, however, immediately reveals how this excitation can be understood as electronic coupling between four different localised $\pi \rightarrow \pi^*$ excitations on each of the four different chromophores. In systems not displaying excitonic character, a single occupied $\rightarrow$ virtual transition in the NTO basis often accounts for $\gtrsim 95\%$ of the total excitation amplitude.

9. Graphical user interfaces

9.1. IQMOL

IQMOL is an open source molecular editor and visualisation package that has been written to work with the Q-CHEM package. It provides a single integrated environment for building molecules, setting up and submitting Q-CHEM calculations, and analysing the resulting output.

IQMOL has a flexible and easy to use free-form molecular builder that allows structures to be built from a variety of building blocks including atoms, functional groups, and entire molecular fragments. It also allows the user to add EFP fragments for use in EFP calculations [413]. The func-

tional groups, molecular fragments, and EFPs are obtained from an internal library that is loaded at start up and that can be easily extended by the user. Structures can be optimised using a range of MM force fields available in the Open Babel library [414] including MMFF94, UFF, Ghemical, and GAFF. Constraints can be applied to the structure and these are applied in the MM minimisation as well as being passed through to Q-CHEM for any subsequent geometry optimisation. Structures can also be symmetrised using the integrated SYMMOL [415] routine which recovers the full point-group symmetry of the molecule to within a given tolerance.

Q-CHEM jobs can be configured using the built-in job set up panel which includes most of the Q-CHEM job options presented in a logical and hierarchical way. Each option has a separate control which has tool-tip documentation associated with it which summarises its use and details what settings are valid, thus reducing the need to constantly check the Q-CHEM user's manual. Multiple Q-CHEM servers can be configured, allowing jobs to be submitted directly from IQMOL. These servers can correspond to either the local machine or a remote server running PBS or SGE queueing software. In the case of remote servers, all communication is carried out securely via SSH channels. Apart from ensuring Q-CHEM is properly installed, no other server-side configuration is required for job submission from IQMOL, allowing it to be used on servers where the user has limited access permissions.

IQMOL's analysis package can read data from a variety of file formats including Q-CHEM input/output, xyz, formatted checkpoint, and cube data files. Isovalue surfaces can be plotted for a range of properties based on an SCF wave function including densities, spin-densities, and MOs. Promolecule and van der Waals surfaces are also available for systems where the wave function information is not available. All surfaces can be coloured based on a scalar property such as the electrostatic potential, or arbitrary data from a cube file. The animation module is capable of animating vibrational frequencies as well as IRC and optimisation pathways. Animations of molecular surfaces are also possible. Key frames are loaded from separate cube files and then a configurable number of interpolated surfaces are generated to provide a smooth transition between the key frames. Animations can be recorded and saved as a movie file for later viewing.

9.2. Spartan

Starting in 2000, Q-CHEM has provided back-end source code to Wavefunction Inc (www.wavefun.com) that provides high performance SCF-level and correlated calculations as part of its advanced user interface within the Spartan Pro and Spartan Student packages. The Spartan environment includes not only highly developed graphics, but also advanced database capabilities and a rich suite of

conformational searching and modelling tools that complement Q-CHEM's focus on *ab initio* methods.

9.3. Other interfaces

Q-CHEM is also interfaced with a variety of other public domain user interfaces, including CHARMMing [300] Avogadro [416], Molden [417], and WebMO [418].

10. Summary

In this review, we have summarised the main technical features that have been incorporated into the Q-CHEM program since the last major review of its capabilities [17]. The main reason that such an extensive range of developments can be reported is the size and level of activity of our developer community, as captured by the authorship list of the paper. Looking to the future, Q-CHEM will continue to try to serve the academic needs of our developers by providing a state of the art development platform, which in turn serves the needs of our users by the creation of new electronic structure capabilities and algorithms. With our open team-ware model, we continue to encourage new developers to join us in creating future advances.

References

[1] G.T. Velde, F.M. Bickelhaupt, E.J. Baerends, C.F. Guerra, S.J.A. Van Gisbergen, J.G. Snijders, and T. Ziegler, J. Comput. Chem. **22**, 931 (2001).

[2] M.J. Frisch, G.W. Trucks, H.B. Schlegel, G.E. Scuseria, M.A. Robb, J.R. Cheeseman, G. Scalmani, V. Barone, B. Mennucci, G.A. Petersson, H. Nakatsuji, M. Caricato, X. Li, H.P. Hratchian, A.F. Izmaylov, J. Bloino, G. Zheng, J.L. Sonnenberg, M. Hada, M. Ehara, K. Toyota, R. Fukuda, J. Hasegawa, M. Ishida, T. Nakajima, Y. Honda, O. Kitao, H. Nakai, T. Vreven, J.A. Montgomery, Jr., J.E. Peralta, F. Ogliaro, M. Bearpark, J.J. Heyd, E. Brothers, K.N. Kudin,

V.N. Staroverov, T. Keith, R. Kobayashi, J. Normand, K. Raghavachari, A. Rendell, J.C. Burant, S.S. Iyengar, J. Tomasi, M. Cossi, N. Rega, J.M. Millam, M. Klene, J.E. Knox, J.B. Cross, V. Bakken, C. Adamo, J. Jaramillo, R. Gomperts, R.E. Stratmann, O. Yazyev, A.J. Austin, R. Cammi, C. Pomelli, J.W. Ochterski, R.L. Martin, K. Morokuma, V.G. Zakrzewski, G.A. Voth, P. Salvador, J.J. Dannenberg, S. Dapprich, A.D. Daniels, O. Farkas, J.B. Foresman, J.V. Ortiz, J. Cioslowski, and D.J. Fox, Gaussian 09, Revision B.01 (2009).

[3] A.D. Bochevarov, E. Harder, T.F. Hughes, J.R. Greenwood, D.A. Braden, D.M. Philipp, D. Rinaldo, M.D. Halls, J. Zhang, and R.A. Friesner, Int. J. Quantum Chem. **113**, 2110 (2013).

[4] F. Aquilante, T.B. Pedersen, V. Veryazov, and R. Lindh, Wiley Interdiscip. Rev. **3**, 143 (2013).

[5] H.J. Werner, P.J. Knowles, G. Knizia, F.R. Manby, and M. Schutz, WIREs Comput. Mol. Sci. **2**, 242 (2012).

[6] R. Ahlrichs, M. Bär, M. Häser, H. Horn, and C. Kölmel, Chem. Phys. Lett. **162**, 165 (1989).

[7] F. Furche, R. Ahlrichs, C. Hättig, W. Klopper, M. Sierka, and F. Weigend, Wiley Interdiscip. Rev. **4**, 91 (2014).

[8] V. Lotrich, N. Flocke, M. Ponton, A.D. Yau, A. Perera, E. Deumens, and R.J. Bartlett, J. Chem. Phys. **128**, 194104 (2008).

[9] M.E. Harding, T. Metzroth, J. Gauss, and A.A. Auer, J. Chem. Theory Comput. **4**, 64 (2008).

[10] K. Aidas, C. Angeli, K.L. Bak, V. Bakken, R. Bast, L. Boman, O. Christiansen, R. Cimiraglia, S. Coriani, P. Dahle, E.K. Dalskov, U. Ekström, T. Enevoldsen, J.J. Eriksen, P. Ettenhuber, B. Fernández, L. Ferrighi, H. Fliegl, L. Frediani, K. Hald, A. Halkier, C. Hättig, H. Heiberg, T. Helgaker, A.C. Hennum, H. Hettema, E. Hjertenaes, S. Høst, I.-M. Høyvik, M.F. Iozzi, B. Jansík, H.J.A. Jensen, D. Jonsson, P. Jørgensen, J. Kauczor, S. Kirpekar, T. Kjaergaard, W. Klopper, S. Knecht, R. Kobayashi, H. Koch, J. Kongsted, A. Krapp, K. Kristensen, A. Ligabue, O.B. Lutnaes, J.I. Melo, K.V. Mikkelsen, R.H. Myhre, C. Neiss, C.B. Nielsen, P. Norman, J. Olsen, J.M.H. Olsen, A. Osted, M.J. Packer, F. Pawlowski, T.B. Pedersen, P.F. Provasi, S. Reine, Z. Rinkevicius, T.A. Ruden, K. Ruud, V.V. Rybkin, P. Sałek, C.C.M. Samson, A.S. de Merás, T. Saue, S.P.A. Sauer, B. Schimmelpfennig, K. Sneskov, A.H. Steindal, K.O. Sylvester-Hvid, P.R. Taylor, A.M. Teale, E.I Tellgren, D.P. Tew, A.J. Thorvaldsen, L. Thøgersen, O. Vahtras, M.A. Watson, D.J.D. Wilson, M. Ziolkowski, and H. Ågren, Wiley Interdiscip. Rev. **4**, 269 (2014).

[11] M.W. Schmidt, K.K. Baldridge, J.A. Boatz, S.T. Elbert, M.S. Gordon, J.H. Jensen, S. Koseki, N. Matsunaga, K.A. Nguyen, S. Su, T.L. Windus, M. Dupuis, and J.A. Montgomery, Jr., J. Comput. Chem. **14**, 1347 (1983).

[12] M.F. Guest, I.J. Bush, H.J.J. Van Dam, P. Sherwood, J.M.H. Thomas, J.H. Van Lenthe, R.W.A. Havenith, and J. Kendrick, Mol. Phys. **103**, 719 (2005).

[13] M. Valiev, E.J. Bylaska, N. Govind, K. Kowalski, T.P. Straatsma, H.J.J. Van Dam, D. Wang, J. Nieplocha, E. Apra, T.L. Windus, and W. de Jong, Comput. Phys. Commun. **181**, 1477 (2010).

[14] J.M. Turney, A.C. Simmonett, R.M. Parrish, E.G. Hohenstein, F.A. Evangelista, J.T. Fermann, B.J. Mintz, L.A. Burns, J.J. Wilke, M.L. Abrams, N.J. Russ, M.L. Leininger, C.L. Janssen, E.T. Seidl, W.D. Allen, H.F. Schaefer, R.A. King, E.F. Valeev, C.D. Sherrill, and T.D. Crawford, WIREs Comput. Mol. Sci. **2**, 556 (2012).

[15] J. Kong, C.A. White, A.I. Krylov, D. Sherrill, R.D. Adamson, T.R. Furlani, M.S. Lee, A.M. Lee, S.R. Gwaltney, T.R. Adams, C. Ochsenfeld, A.T.B. Gilbert, G.S. Kedziora, V.A. Rassolov, D.R. Maurice, N. Nair, Y.H. Shao, N.A. Besley, P.E. Maslen, J.P. Dombroski, H. Daschel, W.M. Zhang, P.P. Korambath, J. Baker, E.F.C. Byrd, T. Van Voorhis, M. Oumi, S. Hirata, C.P. Hsu, N. Ishikawa, J. Florian, A. Warshel, B.G. Johnson, P.M.W. Gill, M. Head-Gordon, and J.A. Pople, J. Comput. Chem. **21**, 1532 (2000).

[16] J.A. Pople, Rev. Mod. Phys. **71**, 1267 (1999).

[17] Y. Shao, L. Fusti-Molnar, Y. Jung, J. Kussmann, C. Ochsenfeld, S.T. Brown, A.T.B. Gilbert, L.V. Slipchenko, S.V. Levchenko, D.P. O'Neill, R.A. DiStasio, Jr., R.C. Lochan, T. Wang, G.J.O. Beran, N.A. Besley, J.M. Herbert, C.Y. Lin, T. Van Voorhis, S.H. Chien, A. Sodt, R.P. Steele, V.A. Rassolov, P.E. Maslen, P.P. Korambath, R.D. Adamson, B. Austin, J. Baker, E.F.C. Byrd, H. Dachsel, R.J. Doerksen, A. Dreuw, B.D. Dunietz, A.D. Dutoi, T.R. Furlani, S.R. Gwaltney, A. Heyden, S. Hirata, C.-P. Hsu, G. Kedziora, R.Z. Khaliullin, P. Klunzinger, A.M. Lee, M.S. Lee, W. Liang, I. Lotan, N. Nair, B. Peters, E.I. Proynov, P.A. Pieniazek, Y.M. Rhee, J. Ritchie, E. Rosta, C.D. Sherrill, A.C. Simmonett, J.E. Subotnik, H.L. Woodcock III, W. Zhang, A.T. Bell, A.K. Chakraborty, D.M. Chipman, F.J. Keil, A. Warshel, W.J. Hehre, H.F. Schaefer III, J. Kong, A.I. Krylov, P.M.W. Gill, and M. Head-Gordon, Phys. Chem. Chem. Phys. **8**, 3172 (2006).

[18] A.I. Krylov and P.M.W. Gill, WIREs Comput. Mol. Sci. **3**, 317 (2013).

[19] W. Kohn, A.D. Becke, and R.G. Parr, J. Phys. Chem. **100**, 12974 (1996).

[20] L. Goerigk and S. Grimme, Phys. Chem. Chem. Phys. **13**, 6670 (2011).

[21] N. Mardirossian, J.A. Parkhill, and M. Head-Gordon, Phys. Chem. Chem. Phys. **13**, 19325 (2011).

[22] R. Sedlak, T. Janowski, M. Pitonak, J. Rezac, P. Pulay, and P. Hobza, J. Chem. Theory Comput. **9**, 3364 (2013).

[23] R. Peverati and D.G. Truhlar, Philos. Trans. R. Soc. A **372**, 20120476 (2014).

[24] J.P. Perdew, A. Ruzsinszky, L.A. Constantin, J.W. Sun, and G.I. Csonka, J. Chem. Theory Comput. **5**, 902 (2009).

[25] A.J. Cohen, P. Mori-Sanchez, and W.T. Yang, Chem. Rev. **112**, 289 (2012).

[26] A.D. Becke, J. Chem. Phys. **98**, 1372 (1993).

[27] Y. Zhao and D.G. Truhlar, Theor. Chem. Acc. **120**, 215 (2008).

[28] R. Peverati and D.G. Truhlar, J. Phys. Chem. Lett. **2**, 2810 (2011).

[29] R. Peverati and D.G. Truhlar, J. Phys. Chem. Lett. **3**, 117 (2012).

[30] J. Tao, J.P. Perdew, V.N. Staroverov, and G.E. Scuseria, Phys. Rev. Lett. **91**, 146401 (2003).

[31] T. Bally and G.N. Sastry, J. Phys. Chem. A **101**, 7923 (1997).

[32] A.D. Dutoi and M. Head-Gordon, Chem. Phys. Lett. **422**, 230 (2006).

[33] A. Dreuw, J.L. Weisman, and M. Head-Gordon, J. Chem. Phys. **119**, 2943 (2003).

[34] A. Dreuw and M. Head-Gordon, J. Am. Chem. Soc. **126**, 4007 (2004).

[35] T.M. Henderson, B.G. Janesko, and G.E. Scuseria, J. Chem. Phys. **128**, 194105 (2008).

[36] M.A. Rohrdanz and J.M. Herbert, J. Chem. Phys. **129**, 034107 (2008).

[37] M.A. Rohrdanz, K.M. Martins, and J.M. Herbert, J. Chem. Phys. **130**, 054112 (2009).

[38] A.W. Lange and J.M. Herbert, J. Am. Chem. Soc. **131**, 124115 (2009).

[39] J.-D. Chai and M. Head-Gordon, J. Chem. Phys. **128**, 084106 (2008).

[40] J.-D. Chai and M. Head-Gordon, Phys. Chem. Chem. Phys. **10**, 6615 (2008).

[41] J.-D. Chai and M. Head-Gordon, J. Chem. Phys. **131**, 174105 (2009).

[42] N. Mardirossian and M. Head-Gordon, Phys. Chem. Chem. Phys. **16**, 9904 (2014).

[43] R. Baer and D. Neuhauser, Phys. Rev. Lett. **94**, 043002 (2005).

[44] E. Livshits and R. Baer, Phys. Chem. Chem. Phys. **9**, 2932 (2007).

[45] U. Salzner and R. Baer, J. Chem. Phys. **131**, 231101 (2009).

[46] R. Baer, E. Livshits, and U. Salzner, Annu. Rev. Phys. Chem. **61**, 85 (2010).

[47] Y. Zhao, N.E. Schultz, and D.G. Truhlar, J. Chem. Theory Comput. **2**, 364 (2006).

[48] N.A. Besley, M.J.G. Peach, and D.J. Tozer, Phys. Chem. Chem. Phys. **11**, 10350 (2009).

[49] S. Kristyan and P. Pulay, Chem. Phys. Lett. **229**, 175 (1994).

[50] J. Klimes and A. Michaelides, J. Chem. Phys. **137**, 120901 (2012).

[51] S. Grimme, J. Comput. Chem. **27**, 1787 (2006).

[52] S. Grimme, J. Antony, S. Ehrlich, and H. Krieg, J. Chem. Phys. **132**, 154104 (2010).

[53] A.D. Becke and E.R. Johnson, J. Chem. Phys. **122**, 154104 (2005).

[54] E.R. Johnson and A.D. Becke, J. Chem. Phys. **123**, 024101 (2005).

[55] J. Kong, Z. Gan, E. Proynov, M. Freindorf, and T. Furlani, Phys. Rev. A **79**, 042510 (2009).

[56] M. Dion, H. Rydberg, E. Schröder, D.C. Langreth, and B.I. Lundqvist, Phys. Rev. Lett. **92**, 246401 (2004).

[57] K. Lee, É.D. Murray, L. Kong, B.I. Lundqvist, and D.C. Langreth, Phys. Rev. B **82**, 081101 (2010).

[58] O.A. Vydrov and T. Van Voorhis, Phys. Rev. Lett. **103**, 063004 (2009).

[59] O.A. Vydrov and T. Van Voorhis, J. Chem. Phys. **133**, 244103 (2010).

[60] S. Grimme, J. Chem. Phys. **124**, 034108 (2006).

[61] T. Schwabe and S. Grimme, Phys. Chem. Chem. Phys. **9**, 3397 (2007).

[62] Y. Zhang, X. Xu, and W.A. Goddard III, Proc. Natl. Acad. Sci. U.S.A. **106**, 4963 (2009).

[63] J.D. Chai and S.P. Mao, Chem. Phys. Lett. **538**, 121 (2012).

[64] I. Zhang, X. Xu, Y. Jung, and W. Goddard, Proc. Natl. Acad. Sci. U.S.A. **108**, 19896 (2011).

[65] H. Ji, Y. Shao, W.A. Goddard, and Y. Jung, J. Chem. Theory Comput. **9**, 1971 (2013).

[66] A.D. Becke, J. Chem. Phys. **119**, 2972 (2003).

[67] A.D. Becke, J. Chem. Phys. **122**, 064101 (2005).

[68] A.D. Becke and M.R. Roussel, Phys. Rev. A **39**, 3761 (1989).

[69] A.D. Becke, J. Chem. Phys. **88**, 1053 (1988).

[70] A.D. Becke, Int. J. Quantum Chem. **52**, 625 (1994).

[71] E. Proynov, Y. Shao, and J. Kong, Chem. Phys. Lett. **493**, 381 (2010).

[72] E. Proynov, F. Liu, Y. Shao, and J. Kong, J. Chem. Phys. **136**, 034102 (2012).

[73] N. Mardirossian and M. Head-Gordon, J. Chem. Phys. **140**, 18A527 (2014).

[74] A. Karton, S. Daon, and J.M. Martin, Chem. Phys. Lett. **510**, 165 (2011).

[75] A. Karton, D. Gruzman, and J.M.L. Martin, J. Phys. Chem. A **113**, 8434 (2009).

[76] J. Zheng, Y. Zhao, and D.G. Truhlar, J. Chem. Theory Comput. **3**, 569 (2007).

[77] A. Karton, A. Tarnopolsky, J.-F. Lamère, G.C. Schatz, and J.M.L. Martin, J. Phys. Chem. A **112**, 12868 (2008).

[78] J. Zheng, Y. Zhao, and D.G. Truhlar, J. Chem. Theory Comput. **5**, 808 (2009).

[79] L.A. Curtiss, K. Raghavachari, G.W. Trucks, and J.A. Pople, J. Chem. Phys. **94**, 7221 (1991).

[80] L. Goerigk and S. Grimme, Phys. Chem. Chem. Phys. **13**, 6670 (2011).

[81] K.L. Copeland and G.S. Tschumper, J. Chem. Theory Comput. **8**, 1646 (2012).

[82] P. Jurečka, J. Šponer, J. Černý, and P. Hobza, Phys. Chem. Chem. Phys. **8**, 1985 (2006).

[83] T. Takatani, E.G. Hohenstein, M. Malagoli, M.S. Marshall, and C.D. Sherrill, J. Chem. Phys. **132**, 144104 (2010).

[84] J. Řezác, K.E. Riley, and P. Hobza, J. Chem. Theory Comput. **7**, 2427 (2011).

[85] J. Řezác, K.E. Riley, and P. Hobza, J. Chem. Theory Comput. **7**, 3466 (2011).

[86] J. Řezáč and P. Hobza, J. Chem. Theory Comput. **9**, 2151 (2013).

[87] J. Řezáč, K.E. Riley, and P. Hobza, J. Chem. Theory Comput. **8**, 4285 (2012).

[88] B.J. Mintz and J.M. Parks, J. Phys. Chem. A **116**, 1086 (2012).

[89] J. Kussmann, M. Beer, and C. Ochsenfeld, Wiley Interdiscip. Rev. **3**, 614 (2013).

[90] C. Ochsenfeld, J. Kussmann, and F. Koziol, Angew. Chem. **43**, 4485 (2004).

[91] W. Pisula, Z. Tomovic, M.D. Watson, K. Müllen, J. Kussmann, C. Ochsenfeld, T. Metzroth, and J. Gauss, J. Phys. Chem. B **111**, 7481 (2007).

[92] D. Flaig, M. Beer, and C. Ochsenfeld, J. Chem. Theory Comput. **8**, 2260 (2012).

[93] J. Kussmann and C. Ochsenfeld, J. Chem. Phys. **127**, 054103 (2007).

[94] C. Ochsenfeld, J. Kussmann, and F. Koziol, Angew. Chem. **116**, 4585 (2004).

[95] S.P. Karna and M. Dupuis, J. Comput. Chem. **12**, 487 (1991).

[96] H. Sekino and R.J. Bartlett, J. Chem. Phys. **98**, 3022 (1993).

[97] J. Kussmann and C. Ochsenfeld, J. Chem. Phys. **127**, 204103 (2007).

[98] C.A. White, B.G. Johnson, P.M.W. Gill, and M. Head-Gordon, Chem. Phys. Lett. **230**, 8 (1994).

[99] C. Ochsenfeld, C.A. White, and M. Head-Gordon, J. Chem. Phys. **109**, 1663 (1998).

[100] C. Ochsenfeld, Chem. Phys. Lett. **327**, 216 (2000).

[101] C.V. Sumowski and C. Ochsenfeld, J. Phys. Chem. A **113**, 11734 (2009).

[102] C.V. Sumowski, B.B.T. Schmitt, S. Schweizer, and C. Ochsenfeld, Angew. Chem. **122**, 10147 (2010).

[103] T. Helgaker, M. Watson, and N.C. Handy, J. Chem. Phys. **113**, 9402 (2000).

[104] V. Sychrovsky, J. Gräfenstein, and D. Cremer, J. Chem. Phys. **113**, 3530 (2000).

[105] A. Luenser, J. Kussmann, and C. Ochsenfeld, 2014, (unpublished).

[106] S.N. Maximoff, J.E. Peralta, V. Barone, and G.E. Scuseria, J. Chem. Theory Comput. **1**, 541 (2005).

[107] T. Bally and P.R. Rablen, J. Org. Chem. **76**, 4818 (2011).

[108] P.F. Provasi, G.A. Aucar, and S.P.A. Sauer, J. Chem. Phys. **115**, 1324 (2001).

[109] F. Jensen, J. Chem. Theory Comput. **2**, 1360 (2006).

[110] F. Jensen, Theor. Chem. Acc. **126**, 371 (2009).

[111] U. Benedikt, A.A. Auer, and F. Jensen, J. Chem. Phys. **129**, 064111 (2008).

[112] N. Matsumori, D. Kaneno, M. Murata, H. Nakamura, and K. Tachibana, J. Org. Chem. **64**, 866 (1999).

[113] G. Bifulco, P. Dambruoso, L. Gomez-Paloma, and R. Riccio, Chem. Rev. **107**, 3744 (2007).

[114] M. Karplus, J. Chem. Phys. **30**, 11 (1959).

[115] M. Karplus, J. Phys. Chem. **64**, 1793 (1960).

[116] M. Karplus, J. Am. Chem. Soc. **85**, 2870 (1963).

[117] M. Barfield and B. Chakrabarti, Chem. Rev. **69**, 757 (1969).

[118] A.J. Dingley, F. Cordier, and S. Grzesiek, Concepts Magn. Res. **13**, 103 (2001).

[119] A. Sodt and M. Head-Gordon, J. Chem. Phys. **125**, 074116 (2006).

[120] A. Sodt and M. Head-Gordon, J. Chem. Phys. **128**, 104106 (2008).

[121] J. Kong, S.T. Brown, and L. Fusti-Molnar, J. Chem. Phys. **124**, 094109 (2006).

[122] C.-M. Chang, N.J. Russ, and J. Kong, Phys. Rev. A **84**, 022504 (2011).

[123] N.J. Russ, C.-M. Chang, and J. Kong, Can. J. Chem. **89**, 657 (2011).

[124] L. Fusti-Molnar and J. Kong, J. Chem. Phys. **122**, 074108 (2005).

[125] S. Hirata and M. Head-Gordon, Chem. Phys. Lett. **314**, 291 (1999).

[126] F. Liu, Z. Gan, Y. Shao, C.-P. Hsu, A. Dreuw, M. Head-Gordon, B.T. Miller, B.R. Brooks, J.-G. Yu, T.R. Furlani, and J. Kong, Mol. Phys. **108**, 2791 (2010).

[127] D. Maurice and M. Head-Gordon, Mol. Phys. **96**, 1533 (1999).

[128] J. Liu and W. Liang, J. Chem. Phys. **135**, 014113 (2011).

[129] J. Liu and W. Liang, J. Chem. Phys. **135**, 184111 (2011).

[130] J. Liu and W. Liang, J. Chem. Phys. **138**, 024101 (2013).

[131] W.Z. Liang and M. Head-Gordon, J. Phys. Chem. A **108**, 3206 (2004).

[132] R.P. Steele, Y. Shao, R.A. DiStasio, Jr., and M. Head-Gordon, J. Phys. Chem. A **110**, 13915 (2006).

[133] R.P. Steele, R.A. DiStasio, Jr., Y. Shao, J. Kong, and M. Head-Gordon, J. Chem. Phys. **125**, 074108 (2006).

[134] R.P. Steele, R.A. DiStasio, Jr., and M. Head-Gordon, J. Chem. Theory Comput. **5**, 1560 (2009).

[135] J. Deng, A.T.B. Gilbert, and P.M.W. Gill, J. Chem. Phys. **130**, 231101 (2009).

[136] J. Deng, A.T.B. Gilbert, and P.M.W. Gill, J. Chem. Phys. **133**, 044116 (2009).

[137] J. Deng, A.T.B. Gilbert, and P.M.W. Gill, Phys. Chem. Chem. Phys. **12**, 10759 (2010).

[138] A.J.W. Thom and M. Head-Gordon, Phys. Rev. Lett. **101**, 193001 (2008).

[139] A.J.W. Thom and M. Head-Gordon, J. Chem. Phys. **131**, 124113 (2009).

[140] E.J. Sundstrom and M. Head-Gordon, J. Chem. Phys. **140**, 114103 (2014).

[141] K.U. Lao and J.M. Herbert, J. Chem. Phys. **139**, 034107 (2013).

[142] C. Møller and M.S. Plesset, Phys. Rev. **46**, 618 (1934).

[143] J.A. Pople, J.S. Binkley, and R. Seeger, Int. J. Quantum Chem. **S10**, 1 (1976).

[144] Y.M. Rhee, R.A. DiStasio, Jr., R.C. Lochan, and M. Head-Gordon, Chem. Phys. Lett. **426**, 197 (2006).

[145] R.A. DiStasio, Jr., R.P. Steele, Y.M. Rhee, Y. Shao, and M. Head-Gordon, J. Comput. Chem. **28**, 839 (2007).

[146] R.A. DiStasio, Jr., R.P. Steele, and M. Head-Gordon, Mol. Phys. **105**, 27331 (2007).

[147] J. Zienau, L. Clin, B. Doser, and C. Ochsenfeld, J. Chem. Phys. **130**, 204112 (2009).

[148] S.A. Maurer, L. Clin, and C. Ochsenfeld, J. Chem. Phys. **140**, 224112 (2014).

[149] S.A. Maurer, D.S. Lambrecht, D. Flaig, and C. Ochsenfeld, J. Chem. Phys. **136**, 144107 (2012).

[150] S.A. Maurer, D.S. Lambrecht, J. Kussmann, and C. Ochsenfeld, J. Chem. Phys. **138**, 014101 (2013).

[151] M. Goldey and M. Head-Gordon, J. Phys. Chem. Lett. **3**, 3592 (2012).

[152] M. Goldey, A. Dutoi, and M. Head-Gordon, Phys. Chem. Chem. Phys. **15**, 15869 (2013).

[153] M. Goldey, R.A. Distasio, Jr., Y. Shao, and M. Head-Gordon, Mol. Phys. **112**, 836 (2014).

[154] B.J. Mintz and J.M. Parks, J. Phys. Chem. A **116**, 1086 (2012).

[155] D.S. Lambrecht, G.N.I. Clark, T. Head-Gordon, and M. Head-Gordon, J. Phys. Chem. A **115**, 11438 (2011).

[156] D.S. Lambrecht, L. McCaslin, S.S. Xantheas, E. Epifanovsky, and M. Head-Gordon, Mol. Phys. **110**, 2513 (2012).

[157] N. Mardirossian, D.S. Lambrecht, L. McCaslin, S.S. Xantheas, and M. Head-Gordon, J. Chem. Theory Comput. **9**, 1368 (2013).

[158] D. Gruzman, A. Karton, and J.M.L. Martin, J. Phys. Chem. A **113**, 11974 (2009).

[159] J.J. Wilke, M.C. Lind, H.F. Schaefer, A.G. Csaszar, and W.D. Allen, J. Chem. Theory Comput. **5**, 1511 (2009).

[160] G.I. Csonka, A.D. French, G.P. Johnson, and C.A. Stortz, J. Chem. Theory Comput. **5**, 679 (2009).

[161] R. Sedlak, T. Janowski, M. Pitoňák, J. Rezac, P. Pulay, and P. Hobza, J. Chem. Theory Comput. **9**, 3364 (2013).

[162] H. Valdes, K. Pluhackova, M. Pitoňák, J. Řezáč, and P. Hobza, Phys. Chem. Chem. Phys. **10**, 2747 (2008).

[163] J. Řezáč, P. Jurecka, K.E. Riley, J. Cerny, H. Valdes, K. Pluhackova, K. Berka, T. Řezáč, M. Pitoňák, J. Vondrasek, and P. Hobza, Collect. Czech. Chem. C **73**, 1261 (2008).

[164] J. Řezáč and P. Hobza, J. Chem. Theory Comput. **9**, 2151 (2013).

[165] R.C. Lochan and M. Head-Gordon, J. Chem. Phys. **126**, 164101 (2007).

[166] W. Kurlancheek, R. Lochan, K. Lawler, and M. Head-Gordon, J. Chem. Phys. **136**, 054113 (2012).

[167] Y. Jung, R.C. Lochan, A.D. Dutoi, and M. Head-Gordon, J. Chem. Phys. **121**, 9793 (2004).

[168] W. Kurlancheek and M. Head-Gordon, Mol. Phys. **107**, 1223 (2009).

[169] D. Stück and M. Head-Gordon, J. Chem. Phys. **139**, 244109 (2013).

[170] M. Head-Gordon, R.J. Rico, M. Oumi, and T.J. Lee, Chem. Phys. Lett. **219**, 21 (1994).

[171] Y.M. Rhee and M. Head-Gordon, J. Phys. Chem. A **111**, 5314 (2007).

[172] E. Epifanovsky, D. Zuev, X. Feng, K. Khistyaev, Y. Shao, and A. Krylov, J. Chem. Phys. **139**, 134105 (2013).

[173] D. Casanova, Y.M. Rhee, and M. Head-Gordon, J. Chem. Phys. **128**, 164106 (2008).

[174] Y.M. Rhee, D. Casanova, and M. Head-Gordon, J. Chem. Theor. Comput. **5**, 1224 (2009).

[175] Y.M. Rhee, D. Casanova, and M. Head-Gordon, J. Phys. Chem. A **113**, 10564 (2009).

[176] R.J. Bartlett and M. Musial, Rev. Mod. Phys. **79**, 291 (2007).

[177] A.I. Krylov, Annu. Rev. Phys. Chem. **59**, 433 (2008).

[178] T. Kuś and A.I. Krylov, J. Chem. Phys. **135**, 084109 (2011).

[179] A.I. Krylov, Acc. Chem. Res. **39**, 83 (2006).

[180] D. Casanova, L.V. Slipchenko, A.I. Krylov, and M. Head-Gordon, J. Chem. Phys. **130**, 044103 (2009).

[181] E. Epifanovsky, M. Wormit, T. Kuś, A. Landau, D. Zuev, K. Khistyaev, P. Manohar, I. Kaliman, A. Dreuw, and A. Krylov, J. Comput. Chem. **34**, 2293 (2013).

[182] A. Landau, K. Khistyaev, S. Dolgikh, and A.I. Krylov, J. Chem. Phys. **132**, 014109 (2010).

[183] T.-C. Jagau, K.B. D. Zuev, E. Epifanovsky, and A. Krylov, J. Phys. Chem. Lett. **5**, 310 (2014).

[184] K.B. Bravaya, D. Zuev, E. Epifanovsky, and A.I. Krylov, J. Chem. Phys. **138**, 124106 (2013).

[185] D. Zuev, T.-C. Jagau, K. Bravaya, E. Epifanovsky, Y. Shao, E. Sundstrom, M. Head-Gordon, and A. Krylov, J. Chem. Phys. **141**, 024102 (2014).

[186] T. Kuś and A.I. Krylov, J. Chem. Phys. **136**, 244109 (2012).

[187] J. Schirmer, Phys. Rev. A **26**, 2395 (1982).

[188] A.B. Trofimov, G. Stelter, and J. Schirmer, J. Chem. Phys. **111**, 9982 (1999).

[189] O. Christiansen, H. Koch, and P. Jørgensen, Chem. Phys. Lett. **243**, 409 (1995).

[190] C. Hättig and F. Weigend, J. Chem. Phys. **113**, 5154 (2000).

[191] J.H. Starcke, M. Wormit, J. Schirmer, and A. Dreuw, Chem. Phys. **329**, 39 (2006).

[192] M. Wormit, D.R. Rehn, P.H.P. Harbach, J. Wenzel, C.M. Krauter, E. Epifanovsky, and A. Dreuw, Mol. Phys. **112**, 774 (2014).

[193] S. Knippenberg, D.R. Rehn, M. Wormit, J.H. Starcke, I.L. Rusakova, A.B. Trofimov, and A. Dreuw, J. Chem. Phys. **136**, 064107 (2012).

[194] C.M. Krauter, M. Pernpointner, and A. Dreuw, J. Chem. Phys. **138**, 044107 (2013).

[195] M. Schreiber, M.R. Silva-Junior, S.P.A. Sauer, and W. Thiel, J. Chem. Phys. **128**, 134110 (2008).

[196] L.S. Cederbaum, W. Domcke, and J. Schirmer, Phys. Rev. A **22**, 206 (1980).

[197] J. Wenzel, M. Wormit, and A. Dreuw (2014), J. Comp. Chem. (2014). DOI:10.1002/jcc.23703.

[198] G.K.-L. Chan and M. Head-Gordon, J. Chem. Phys. **116**, 4462 (2002).

[199] G.K.-L. Chan, J. Chem. Phys. **120**, 3172 (2004).

[200] D. Ghosh, J. Hachmann, T. Yanai, and G.K.-L. Chan, J. Chem. Phys. **128**, 144117 (2008).

[201] S. Sharma and G.K.-L. Chan, J. Chem. Phys. **136**, 124121 (2012).

[202] S.R. White, Phys. Rev. Lett. **69**, 2863 (1992).

[203] S.R. White, Phys. Rev. B **48**, 10345 (1993).

[204] S.R. White and R.L. Martin, J. Chem. Phys. **110**, 4127 (1999).

[205] K.H. Marti, I.M. Ondík, G. Moritz, and M. Reiher, J. Chem. Phys. **128**, 014104 (2008).

[206] Ö. Legeza and J. Sólyom, Phys. Rev. B **68**, 195116 (2003).

[207] A. Mitrushenkov, R. Linguerri, P. Palmieri, and G. Fano, J. Chem. Phys. **119**, 4148 (2003).

[208] G.K.-L. Chan and S. Sharma, Annu. Rev. Phys. Chem. **62**, 465 (2011).

[209] D. Zgid and M. Nooijen, J. Chem. Phys. **128**, 144116 (2008).

[210] T. Yanai, Y. Kurashige, D. Ghosh, and G.K. Chan, Int. J. Quantum Chem. **109**, 2178 (2009).

[211] T. Yanai, Y. Kurashige, E. Neuscamman, and G.K.-L. Chan, J. Chem. Phys. **132**, 024105 (2010).

[212] G.K. Chan, Wiley Interdiscip. Rev. **2**, 907 (2012).

[213] G.K.-L. Chan and M. Head-Gordon, J. Chem. Phys. **118**, 8551 (2003).

[214] G.K.-L. Chan, M. Kállay, and J. Gauss, J. Chem. Phys. **121**, 6110 (2004).

[215] S. Sharma, T. Yanai, G.H. Booth, C.J. Umrigar, and G.K.-L. Chan, J. Chem. Phys. **140**, 104112 (2014).

[216] J. Hachmann, J.J. Dorando, M. Avilés, and G.K.-L. Chan, J. Chem. Phys. **127**, 134309 (2007).

[217] Y. Kurashige and T. Yanai, J. Chem. Phys. **135**, 094104 (2011).

[218] Y. Kurashige, G.K.-L. Chan, and T. Yanai, Nature Chem. **5**, 660 (2013).

[219] J. Hachmann, W. Cardoen, and G.K.-L. Chan, J. Chem. Phys. **125**, 144101 (2006).

[220] W. Mizukami, Y. Kurashige, and T. Yanai, J. Chem. Phys. **133**, 091101 (2010).

[221] D. Casanova and M. Head-Gordon, J. Chem. Phys. **129**, 064104 (2008).

[222] P.M. Zimmerman, F. Bell, M. Goldey, A.T. Bell, and M. Head-Gordon, J. Chem. Phys. **137**, 164110 (2012).

[223] D. Casanova, J. Comput. Chem. **34**, 720 (2013).

[224] D. Casanova and M. Head-Gordon, Phys. Chem. Chem. Phys. **11**, 9779 (2009).

[225] F. Bell, P.M. Zimmerman, D. Casanova, M. Goldey, and M. Head-Gordon, Phys. Chem. Chem. Phys. **15**, 358 (2013).

[226] P.M. Zimmerman, F. Bell, D. Casanova, and M. Head-Gordon, J. Am. Chem. Soc. **133**, 19944 (2011).

[227] P. Zimmerman, C. Musgrave, and M. Head-Gordon, Acc. Chem. Res. **46**, 1339 (2013).

[228] X. Feng, A. Luzanov, and A. Krylov, J. Phys. Chem. Lett. **4**, 3845 (2013).

[229] A. Kolomeisky, X. Feng, and A. Krylov, J. Phys. Chem. C **118**, 5188 (2014).

[230] N.J. Mayhall, M. Goldey, and M. Head-Gordon, J. Chem. Theory Comput. **10**, 589 (2014).

[231] N. Mayhall and M. Head-Gordon, J. Chem. Phys. **141**, 044112 (2014).

[232] J. Cullen, Chem. Phys. **202**, 217 (1996).

[233] G.J.O. Beran, B. Austin, A. Sodt, and M. Head-Gordon, J. Phys. Chem. A **109**, 9183 (2005).

[234] D.W. Small and M. Head-Gordon, J. Chem. Phys. **130**, 084103 (2009).

[235] D.W. Small and M. Head-Gordon, Phys. Chem. Chem. Phys. **13**, 19285 (2011).

[236] Y. Kurashige and T. Yanai, J. Chem. Phys. **135**, 094104 (2011).

[237] A.J.H. Wachters, J. Chem. Phys. **52**, 1033 (1970).

[238] A.J.H. Wachters, IBM Technical Report RJ584, 1969.

[239] C.W. Bauschlicher, Jr., S.R. Langhoff, and L.A. Barnes, J. Chem. Phys. **91**, 2399 (1989).

[240] L. Vogt, R. Olivares-Amaya, S. Kermes, Y. Shao, C. Amador-Bedolla, and A. Aspuru-Guzik, J. Phys. Chem. A **112**, 2049 (2008).

[241] M. Watson, R. Olivares-Amaya, R.G. Edgar, and A. Aspuru-Guzik, Comput. Sci. Eng. **12**, 40 (2010).

[242] H. Schlegel, J. Comput. Chem. **24**, 1514 (2003).

[243] A. Banerjee, N. Adams, J. Simons, and R. Shepard, J. Phys. Chem. **89**, 52 (1985).

[244] A. Heyden, A.T. Bell, and F.J. Keil, J. Chem. Phys. **123**, 224101 (2005).

[245] B. Peters, A. Heyden, A.T. Bell, and A. Chakraborty, J. Chem. Phys. **120**, 7877 (2004).

[246] A. Behn, P.M. Zimmerman, A.T. Bell, and M. Head-Gordon, J. Chem. Theory Comput. **7**, 4019 (2011).

[247] T.A. Halgren and W.N. Lipscomb, Chem. Phys. Lett. **49**, 225 (1977).

[248] A. Behn, P.M. Zimmerman, A.T. Bell, and M. Head-Gordon, J. Chem. Phys. **135**, 224108 (2011).

[249] S.M. Sharada, P.M. Zimmerman, A.T. Bell, and M. Head-Gordon, J. Chem. Theory Comput. **8**, 5166 (2012).

[250] J.M. Herbert and M. Head-Gordon, Phys. Chem. Chem. Phys. **7**, 3269 (2005).

[251] E. Ramos-Cordoba, D.S. Lambrecht, and M. Head-Gordon, Faraday Discuss. **150**, 345 (2011).

[252] M. Karplus, R.N. Porter, and R.D. Sharma, J. Chem. Phys. **43**, 3259 (1965).

[253] R. Porter, L. Raff, and W.H. Miller, J. Chem. Phys. **63**, 2214 (1975).

[254] D.S. Lambrecht, G.N.I. Clark, T. Head-Gordon, and M. Head-Gordon, J. Phys. Chem. A **115**, 5928 (2011).

[255] P.M. Zimmerman, D.C. Tranca, J. Gomes, D.S. Lambrecht, M. Head-Gordon, and A.T. Bell, J. Am. Chem. Soc. **134**, 19468 (2012).

[256] D. Wales and J. Doye, J. Phys. Chem. A **101**, 5111 (1997).

[257] H. Do and N.A. Besley, J. Chem. Phys. **137**, 134106 (2012).

[258] H. Do and N.A. Besley, J. Phys. Chem. A **117**, 5385 (2013).

[259] H. Do and N.A. Besley, Phys. Chem. Chem. Phys. **15**, 16214 (2013).

[260] K. Mizuse, J. Kuo, and A. Fujii, Chem. Sci. **2**, 868 (2011).

[261] H.L. Woodcock, M. Hodoscek, A.T.B. Gilbert, P.M.W. Gill, H.F. Schaefer III, and B.R. Brooks, J. Comput. Chem. **28**, 1485 (2007).

[262] B.R. Brooks, C.L. Brooks III, A.D. Mackerell, Jr., L. Nilsson, R.J. Petrella, B. Roux, Y. Won, G. Archontis, C. Bartels, S. Boresch, A. Caflisch, L. Caves, C. Qui, A.R. Dinner, M. Feig, S. Fischer, J. Gao, M. Hodoscek, W. Im, K. Kuczera, T. Lazaridis, J. Ma, V. Ovchinnikov, E. Paci, R.W. Pastor, C.B. Post, J.Z. Pu, M. Schaefer, B. Tidor, R.M. Venable, H.L. Woodcock, X. Wu, W. Yang, D.M. York, and M. Karplus, J. Comput. Chem. **30**, 1545 (2009).

[263] D. Ghosh, D. Kosenkov, V. Vanovschi, C.F. Williams, J.M. Herbert, M.S. Gordon, M.W. Schmidt, L.V. Slipchenko, and A.I. Krylov, J. Phys. Chem. A **114**, 12739 (2010).

[264] L.D. Jacobson, R.M. Richard, K.U. Lao, and J.M. Herbert, Annu. Rep. Comput. Chem. **9**, 25 (2013).

[265] C.J. Cramer and D.G. Truhlar, Chem. Rev. **99**, 2161 (1999).

[266] J. Tomasi, B. Mennucci, and R. Cammi, Chem. Rev. **106**, 2999 (2005).

[267] J. Tomasi, B. Mennucci, and E. Cancès, J. Mol. Struct. (Theochem) **464**, 211 (1999).

[268] D.M. Chipman, Theor. Chem. Acc. **107**, 80 (2002).

[269] D.M. Chipman, J. Chem. Phys. **112**, 5558 (2000).

[270] E. Cancès and B. Mennucci, J. Chem. Phys. **114**, 4744 (2001).

[271] A.W. Lange and J.M. Herbert, Chem. Phys. Lett. **509**, 77 (2011).

[272] V. Barone and M. Cossi, J. Phys. Chem. A **102**, 1995 (1998).

[273] M. Cossi, N. Rega, G. Scalmani, and V. Barone, J. Comput. Chem. **24**, 669 (2003).

[274] T.N. Truong and E.V. Stefanovich, Chem. Phys. Lett. **240**, 253 (1995).

[275] A. Klamt and V. Jonas, J. Chem. Phys. **105**, 9972 (1996).

[276] K. Baldridge and A. Klamt, J. Chem. Phys. **106**, 6622 (1997).

[277] A. Klamt and G. Schüürmann, J. Chem. Soc. Perkin Trans. **2**, 799 (1993).

[278] J.B. Foresman, T.A. Keith, K.B. Wiberg, J. Snoonian, and M.J. Frisch, J. Phys. Chem. **100**, 16098 (1996).

[279] D.M. Chipman and M. Dupuis, Theor. Chem. Acc. **107**, 90 (2002).

[280] V. Barone, M. Cossi, and J. Tomasi, J. Chem. Phys. **107**, 3210 (1997).

[281] A. Pomogaeva and D.M. Chipman, J. Chem. Theory Comput. **7**, 3952 (2011).

[282] A. Pomogaeva and D.M. Chipman, J. Chem. Theory Comput. **10**, 211 (2014).

[283] C.J. Cramer and D.G. Truhlar, Acc. Chem. Res. **41**, 760 (2008).

[284] A.W. Lange and J.M. Herbert, J. Phys. Chem. Lett. **1**, 556 (2010).

[285] A.W. Lange and J.M. Herbert, J. Chem. Phys. **133**, 244111 (2010).

[286] C. Curutchet, M. Orozco, and F.J. Luque, J. Comput. Chem. **22**, 1180 (2001).

[287] I. Soteras, C. Curutchet, A. Bidon-Chanal, M. Orozco, and F.J. Luque, J. Mol. Struct. (Theochem) **727**, 29 (2005).

[288] A. Klamt, B. Mennucci, J. Tomasi, V. Barone, C. Curutchet, M. Orozco, and F.J. Luque, Acc. Chem. Res. **42**, 489 (2009).

[289] W.C. Still, A. Tempczyk, R.C. Hawley, and T. Hendrickson, J. Am. Chem. Soc. **112**, 6127 (1990).

[290] C.J. Cramer and D.G. Truhlar, J. Am. Chem. Soc. **113**, 8305 (1991).

[291] A.V. Marenich, R.M. Olson, C.P. Kelly, C.J. Cramer, and D.G. Truhlar, J. Chem. Theory Comput. **3**, 2011 (2007).

[292] A.V. Marenich, C.J. Cramer, and D.G. Truhlar, J. Chem. Theory Comput. **9**, 609 (2013).

[293] A.V. Marenich, S.V. Jerome, C.J. Cramer, and D.G. Truhlar, J. Chem. Theory Comput. **8**, 527 (2012).

[294] A. Klamt, J. Phys. Chem. **99**, 2225 (1995).

[295] A. Klamt, F. Eckert, and W. Arlt, Annu. Rev. Chem. Biomol. Eng. **1**, 101 (2010).

[296] H.L. Woodcock, W. Zheng, A. Ghysels, Y. Shao, J. Kong, and B.R. Brooks, J. Chem. Phys. **129**, 214109 (2008).

[297] A. Ghysels, H.L. Woodcock, J.D. Larkin, B.T. Miller, Y. Shao, J. Kong, D. Van Neck, V. Van Speybroeck, M. Waroquier, and B.R. Brooks, J. Chem. Theory Comput. **7**, 496 (2011).

[298] T. Benighaus and W. Thiel, J. Chem. Theory Comput. **5**, 3114 (2009).

[299] J. Zienau and Q. Cui, J. Phys. Chem. B **116**, 12522 (2012).

[300] B.T. Miller, R.P. Singh, J.B. Klauda, M. Hodoscek, B.R. Brooks, and H.L. Woodcock III, J. Chem. Inf. Model. **48**, 1920 (2008).

[301] Z.C. Holden, R.M. Richard, and J.M. Herbert, J. Chem. Phys. **139**, 244108 (2013).

[302] J.C. Flick, D. Kosenkov, E.G. Hohenstein, C.D. Sherrill, and L.V. Slipchenko, J. Chem. Theory Comput. **8**, 2835 (2012).

[303] K.U. Lao and J.M. Herbert, J. Phys. Chem. Lett. **3**, 3241 (2012).

[304] K.U. Lao and J.M. Herbert, J. Chem. Phys. **139**, 034107 (2013).

[305] J.M. Herbert and A.W. Lange, in *Many-Body Effects and Electrostatics in Multi-scale Computations of Biomolecules*, edited by Q. Cui, P. Ren, and M. Meuwly (Pan Stanford Publishing Pte. Ltd., Singapore, 2014). (unpublished)

[306] P.N. Day, J.H. Jensen, M.S. Gordon, S.P. Webb, W.J. Stevens, M. Krauss, D. Garmer, H. Basch, and D. Cohen, J. Chem. Phys. **105**, 1968 (1996).

[307] M.S. Gordon, M.A. Freitag, P. Bandyopadhyay, J.H. Jensen, V. Kairys, and W.J. Stevens, J. Phys. Chem. A **105**, 293 (2001).

[308] M.S. Gordon, L.V. Slipchenko, H. Li, and J.H. Jensen, Annu. Rep. Comp. Chem. **3**, 177 (2007).

[309] M.S. Gordon, D.G. Fedorov, S.R. Pruitt, and L.V. Slipchenko, Chem. Rev. **112**, 632 (2012).

[310] L.V. Slipchenko, J. Phys. Chem. A **114**, 8824 (2010).

[311] D. Kosenkov and L.V. Slipchenko, J. Phys. Chem. A **115**, 392 (2011).

[312] D. Ghosh, O. Isayev, L. Slipchenko, and A. Krylov, J. Phys. Chem. A **115**, 6028 (2011).

[313] D. Ghosh, A. Roy, R. Seidel, B. Winter, S. Bradforth, and A. Krylov, J. Phys. Chem. B **116**, 7269 (2012).

[314] M. Gordon and M. Schmidt, in *Advances in Electronic Structure Theory: GAMESS a Decade Later*, edited by C.E. Dykstra, G. Frenking, K.S. Kim, G.E. Scuseria (Elsevier, Amsterdam, 2005), Chap. 41.

[315] I.A. Kaliman and L.V. Slipchenko, J. Comput. Chem. **34**, 2284 (2013).

[316] E. Dahlke and D.G. Truhlar, J. Chem. Theory Comput. **3**, 46 (2007).

[317] C.M. Breneman and K.B. Wiberg, J. Comput. Chem. **11**, 361 (1990).

[318] R.M. Richard and J.M. Herbert, J. Chem. Phys. **137**, 064113 (2012).

[319] L.D. Jacobson and J.M. Herbert, J. Chem. Phys. **134**, 094118 (2011).

[320] J.M. Herbert, L.D. Jacobson, K.U. Lao, and M.A. Rohrdanz, Phys. Chem. Chem. Phys. **14**, 7679 (2012).

[321] B. Jeziorski, R. Moszynski, and K. Szalewicz, Chem. Rev. **94**, 1887 (1994).

[322] J. Řezáč and P. Hobza, J. Chem. Theory Comput. **8**, 141 (2012).

[323] S.A. Maurer, M. Beer, D.S. Lambrecht, and C. Ochsenfeld, J. Chem. Phys. **139**, 184104 (2013).

[324] T. Förster, Ann. Phys. (Leipzig) **2**, 55 (1948).

[325] Z.-Q. You and C.-P. Hsu, J. Phys. Chem. A **115**, 4092 (2011).

[326] M.A. Baldo, S. Lamansky, P.E. Burrows, M.E. Thompson, and S.R. Forrest, Appl. Phys. Lett. **75**, 4 (1999).

[327] H. Yersin, editor, *Highly Efficient OLEDs with Phosphorescent Materials* (Wiley-VCH, Weinheim, 2008).

[328] P.A.M. Dirac, Proc. R. Soc. London A **114**, 243 (1927).

[329] C.-P. Hsu, Z.-Q. You, and H.-C. Chen, J. Phys. Chem. C **112**, 1204 (2008).

[330] C.-P. Hsu, Acc. Chem. Res. **42**, 509 (2009).

[331] Z.-Q. You and C.-P. Hsu, J. Chem. Phys. **133**, 074105 (2010).

[332] Z.-Q. You and C.-P. Hsu, Int. J. Quantum Chem. **114**, 102 (2014).

[333] D.L. Dexter, J. Chem. Phys. **21**, 836 (1953).

[334] R. McWeeny, *Methods of Molecular Quantum Mechanics*, 2nd ed. (Academic Press, New York, 1992).

[335] C.-P. Hsu, G.R. Fleming, M. Head-Gordon, and T. Head-Gordon, J. Chem. Phys. **114**, 3065 (2001).

[336] S.-I. Choi, J. Jortner, S.A. Rice, and R. Silbey, J. Chem. Phys. **41**, 3294 (1964).

[337] R.D. Harcourt, G.D. Scholes, and K.P. Ghiggino, J. Chem. Phys. **101**, 10521 (1994).

[338] M.F. Iozzi, B. Mennucci, J. Tomasi, and R. Cammi, J. Chem. Phys. **120**, 7029 (2004).

[339] G.D. Scholes, C. Curutchet, B. Mennucci, R. Cammi, and J. Tomasi, J. Phys. Chem. B **111**, 6978 (2007).

[340] C. Curutchet, G.D. Scholes, B. Mennucci, and R. Cammi, J. Phys. Chem. B **111**, 13253 (2007).

[341] T. Van Voorhis, T. Kowalczyk, B. Kaduk, L.P. Wang, C.L. Cheng, and Q. Wu, Ann. Rev. Phys. Chem. **61**, 149 (2010).

[342] B. Kaduk, T. Kowalczyk, and T. Van Voorhis, Chem. Rev. **112**, 321 (2012).

[343] P.H. Dederichs, S. Blügel, R. Zeller, and H. Akai, Phys. Rev. Lett. **53**, 2512 (1984).

[344] Q. Wu and T. Van Voorhis, Phys. Rev. A **72**, 024502 (2005).

[345] Q. Wu and T. Van Voorhis, J. Chem. Theory Comput. **2**, 765 (2006).

[346] Q. Wu and T. Van Voorhis, J. Phys. Chem. A **110**, 9212 (2006).

[347] I. Rudra, Q. Wu, and T. Van Voorhis, J. Chem. Phys. **24**, 024103 (2006).

[348] Q. Wu and T. Van Voorhis, J. Chem. Phys. **125**, 164105 (2006).

[349] Q. Wu, C.L. Cheng, and T. Van Voorhis, J. Chem. Phys. **127**, 164119 (2007).

[350] Q. Wu, B. Kaduk, and T. Van Voorhis, J. Chem. Phys. **130**, 034109 (2009).

[351] B. Kaduk and T. Van Voorhis, J. Chem. Phys. **133**, 061102 (2010).

[352] B. Kaduk, T. Tsuchimochi, and T. Van Voorhis, J. Chem. Phys. **140**, 18A503 (2014).

[353] J.E. Subotnik, S. Yeganeh, R.J. Cave, and M.A. Ratner, J. Chem. Phys. **129**, 244101 (2008).

[354] J.E. Subotnik, R.J. Cave, R.P. Steele, and N. Shenvi, J. Chem. Phys. **130**, 234102 (2009).

[355] J.E. Subotnik, J. Vura-Weis, A. Sodt, and M.A. Ratner, J. Phys. Chem. A **114**, 8665 (2010).

[356] J. Vura-Weis, M. Wasielewski, M.D. Newton, and J.E. Subotnik, J. Phys. Chem. C **114**, 20449 (2010).

[357] D.R. Yarkony, *Conical Intersections: Electronic Structure, Dynamics and Spectroscopy* (World Scientific Publishing Co., Singapore, 2004).

[358] S. Fatehi, E. Alguire, Y. Shao, and J.E. Subotnik, J. Chem. Phys. **135**, 234105 (2011).

[359] C.P. Collier, G. Mattersteig, E.W. Wong, Y. Luo, K. Beverly, J. Sampaio, F.M. Raymo, J.F. Stoddart, and J.R. Heath, Science **289**, 1172 (2000).

[360] T. Rueckes, K. Kim, E. Joselevich, G.Y. Tseng, C.L. Cheung, and C.M. Lieber, Science **289**, 94 (2000).

[361] J.M. Tour, A.M. Rawlett, M. Kozaki, Y.X. Yao, R.C. Jagessar, S.M. Dirk, D.W. Price, M.A. Reed, C.W. Zhou, J. Chen, W.Y. Wang, and I. Campbell, Chem.-Eur. J. **7**, 5118 (2001).

[362] F.R.F. Fan, J.P. Yang, L.T. Cai, D.W. Price, S.M. Dirk, D.V. Kosynkin, Y.X. Yao, A.M. Rawlett, J.M. Tour, and A.J. Bard, J. Am. Chem. Soc. **124**, 5550 (2002).

[363] J. Park, A.N. Pasupathy, J.I. Goldsmith, C. Chang, Y. Yaish, J.R. Petta, M. Rinkoski, J.P. Sethna, H.D. Abruna, P.L. McEuen, and D.C. Ralph, Nature **417**, 722 (2002).

[364] W.J. Liang, M.P. Shores, M. Bockrath, J.R. Long, and H. Park, Nature **417**, 725 (2002).

[365] Y. Luo, C.P. Collier, J.O. Jeppesen, K.A. Nielsen, E. Delonno, G. Ho, J. Perkins, H.R. Tseng, T. Yamamoto, J.F. Stoddart, and J.R. Heath, Chem. Phys. Chem. **3**, 519 (2002).

[366] R.M. Metzger, Chem. Rev. **103**, 3803 (2003).

[367] A. Nitzan and M.A. Ratner, Science **300**, 1384 (2003).

[368] W. Tian, S. Datta, S. Hong, R. Reifenberger, J.I. Henderson, and C.P. Kubiak, J. Chem. Phys. **109**, 2874 (1998).

[369] S.N. Yaliraki, A.E. Roitberg, C. Gonzalez, V. Mujica, and M.A. Ratner, J. Chem. Phys. **111**, 6997 (1999).

[370] M. Di Ventra, S.T. Pantelides, and N.D. Lang, Phys. Rev. Lett. **84**, 979 (2000).

[371] Y. Xue, S. Datta, and M.A. Ratner, Chem. Phys. **281**, 151 (2002).

[372] K. Stokbro, J. Taylor, M. Brandbyge, J.L. Mozos, and P. Ordejon, Comput. Mater. Sci. **27**, 151 (2002).

[373] R. Landauer, Philos. Mag. **21**, 863 (1970).

[374] P.F. Bagwell and T.P. Orlando, Phys. Rev. B **40**, 1456 (1989).

[375] Y. Imry and R. Landauer, Rev. Mod. Phys. **71**, S306 (1999).

[376] S. Datta, *Electronic Transport in Mesoscopic Systems* (Cambridge University Press, New York, 1995).

[377] M.P. Samanta, W. Tian, S. Datta, J.I. Henderson, and C.P. Kubiak, Phys. Rev. B **53**, R7626 (1996).

[378] J. Taylor, H. Guo, and J. Wang, Phys. Rev. B **63**, 245407 (2001).

[379] M. Brandbyge, J.L. Mozos, P. Ordejon, J. Taylor, and K. Stokbro, Phys. Rev. B **65**, 165401 (2002).

[380] Y. Chen, A. Prociuk, T. Perrine, and B.D. Dunietz, Phys. Rev. B **74**, 245320 (2006).

[381] M. Das and B.D. Dunietz, J. Phys. Chem. C **111**, 1535 (2007).

[382] T. Perrine and B.D. Dunietz, Phys. Rev. B **75**, 195319 (2007).

[383] T. Perrine and B.D. Dunietz, Nanotechnology **18**, 424003 (2007).

[384] T.M. Perrine, R.G. Smith, C. Marsh, and B.D. Dunietz, J. Chem. Phys. **128**, 154706 (2008).

[385] T. Perrine and B.D. Dunietz, J. Phys. Chem. A **112**, 2043 (2008).

[386] T.M. Perrine, T. Berto, and B.D. Dunietz, J. Phys. Chem. B **112**, 16070 (2008).

[387] Z. Zhao and B.D. Dunietz, J. Chem. Phys. **129**, 024702 (2008).

[388] T. Perrine and B.D. Dunietz, J. Am. Chem. Soc. **132**, 2914 (2010).

[389] B. Ding, V. Washington, and B.D. Dunietz, Mol. Phys. **108**, 2591 (2010).

[390] A. Tan, J. Balachandran, S. Sadat, V. Gavini, B.D. Dunietz, S.-Y. Jang, and P. Reddy, J. Am. Chem. Soc. **133**, 8838 (2011).

[391] R. Balachandran, P. Reddy, B.D. Dunietz, and V. Gavini, J. Phys. Chem. Lett. **3**, 1962 (2012).

[392] R. Balachandran, P. Reddy, B.D. Dunietz, and V. Gavini, J. Phys. Chem. Lett. **4**, 3825 (2013).

[393] A. Prociuk, B. Van Kuiken, and B.D. Dunietz, J. Chem. Phys. **125**, 204717 (2006).

[394] P. Pal and B.D. Dunietz, J. Chem. Phys. **137**, 194104 (2012).

[395] A.E. Reed, R.B. Weinstock, and F. Weinhold, J. Chem. Phys. **83**, 735 (1985).

[396] A.E. Reed, L.A. Curtiss, and F. Weinhold, Chem. Rev. **88**, 899 (1988).

[397] F. Weinhold and C. Landis, *Valency and Bonding: A Natural Bond Orbital Donor-Acceptor Perspective* (Cambridge University Press, Cambridge, 2005), p. 760.

[398] E.D. Glendening, C.R. Landis, and F. Weinhold, WIREs Comput. Mol. Sci. **2**, 1 (2012).

[399] R.Z. Khaliullin, E.A. Cobar, R.C. Lochan, A.T. Bell, and M. Head-Gordon, J. Phys. Chem. A **111**, 8753 (2007).

[400] K. Kitaura and K. Morokuma, Int. J. Quantum Chem. **10**, 325 (1976).

[401] Y.R. Mo, J.L. Gao, and S.D. Peyerimhoff, J. Chem. Phys. **112**, 5530 (2000).

[402] Y. Mo, P. Bao, and J. Gao, Phys. Chem. Chem. Phys. **13**, 6760 (2011).

[403] R.J. Azar, P.R. Horn, E.J. Sundstrom, and M. Head-Gordon, J. Chem. Phys. **138**, 084102 (2013).

[404] P.R. Horn, E.J. Sundstrom, T.A. Baker, and M. Head-Gordon, J. Chem. Phys. **138**, 134119 (2013).

[405] R.Z. Khaliullin, M. Head-Gordon, and A.T. Bell, J. Chem. Phys. **124**, 204105 (2006).

[406] R.Z. Khaliullin, A.T. Bell, and M. Head-Gordon, J. Chem. Phys. **128**, 184112 (2008).

[407] F. Bell, Q.N. Ruan, A. Golan, P.R. Horn, M. Ahmed, S.R. Leone, and M. Head-Gordon, J. Am. Chem. Soc. **135**, 14229 (2013).

[408] M. Head-Gordon, A.M. Grana, D. Maurice, and C.A. White, J. Phys. Chem. **99**, 14261 (1995).

[409] A.V. Luzanov, A.A. Sukhorukov, and V.E. Umanskii, Theor. Exp. Chem. **10**, 354 (1976).

[410] R.L. Martin, J. Chem. Phys. **118**, 4775 (2003).

[411] I. Mayer, Chem. Phys. Lett. **437**, 284 (2007).

[412] H. Shao, J. Seifert, N.C. Romano, M. Gao, J.J. Helmus, C.P. Jaroniec, D.A. Modarelli, and J.R. Parquette, Angew. Chem. **49**, 7688 (2010).

[413] D. Ghosh, D. Kosenkov, V. Vanovschi, J. Flick, I. Kaliman, Y. Shao, A. Gilbert, L. Slipchenko, and A. Krylov, J. Comput. Chem. **34**, 1060 (2013).

[414] N.M. O'Boyle, M. Banck, C.A. James, C. Morley, T. Vandermeersch, and G.R. Hutchison, J. Cheminf. **3**, 33 (2011).

[415] T. Pilati and A. Forni, J. Appl. Cryst. **31**, 503 (1998).

[416] M.D. Hanwell, D.E. Curtis, D.C. Lonie, T. Vandermeersch, E. Zurek, and G.R. Hutchinson, J. Cheminf. **4**, 17 (2012).

[417] G. Schaftenaar and J.H. Noordik, J. Comput.-Aided Mol. Design **14**, 123 (2000).

[418] J.R. Schmidt and W.F. Polik, WebMO Enterprise, version 14.0 (WebMO LLC, Holland, MI, 2014). http://www.webmo.net.